TUNABLE VISIBLE LASER

J. M. Yarborough

GTE Sylvania, Incorporated

Prepared for:

Advanced Research Projects Agency

March 1973

TUNABLE VISIBLE LASER

J. M. Yarborough

GTE Sylvania Inc.
ELECTRO-OPTICS ORGANIZATION
MOUNTAIN VIEW, CALIFORNIA 94040

FINAL REPORT

MARCH 1973

Prepared under contract no. N00014-72-C-0398

SPONSORED BY
ADVANCED RESEARCH PROJECTS AGENCY
ARPA ORDER NO. 1806

TUNABLE VISIBLE LASER

FINAL REPORT

MARCH 1973

ARPA Order Number:	1806
Program Code Number:	2E90
Name of Contractor:	GTE Sylvania, Inc.
Effective Date of Contract:	1 April 1972
Contract Expiration Date:	31 December 1972
Amount of Contract:	$98,783
Contract Number:	N00014-72-C-0398
Principal Investigator:	Dr. J. M. Yarborough
Telephone:	(415)966-3014
Scientific Officer:	Dr. Fred Quelle
Title:	Tunable Visible Laser

Form Approved Budget Bureau Number 22-R0293

Sponsored by

Advanced Research Projects Agency

ARPA Order No. 1806

This research was supported by the Advanced Research Projects Agency of the Department of Defense and was monitored by ONR under Contract Number N00014-72-C-0398.

FOREWORD

This report summarizes the work performed on Office of Naval Research Contract No. N00014-72-C-0398, entitled "High-Power, Tunable, Visible-Laser Source Research". This was an eleven month program to experimentally investigate high average power frequency doubling and quadrupling of Nd:YAG lasers and to demonstrate a high average power tunable visible source by pumping an optical parametric oscillator with the Nd:YAG fourth harmonic. The work summarized in this report covers the period from 1 April 1972 to 28 February 1973. This report was prepared by the Electro-Optics Organization of GTE Sylvania - Western Division, Mountain View, California. Dr. J. M. Yarborough was the principal investigator. Dr. E. O. Ammann and Dr. J. Falk were major contributors. Technical assistance was provided by Messrs. L. H. Martin and J. D. Wintemute.

The work performed under this contract was administered by the Office of Naval Research. Dr. F. Quelle served as the technical officer for ONR.

ABSTRACT

This report summarizes the results of an eleven month research program to efficiently frequency double and quadruple the 1.06 micron output of a Nd:YAG laser and to use the ultraviolet output to pump an optical parametric oscillator tunable throughout the visible spectrum. During this program, average powers of 10 watts at 0.53 micron were obtained from a single CD*A second harmonic generation (SHG) crystal, with greater than 40% conversion from 1.06 micron to 0.53 micron. The green output was in the form of 0.4 joule pulses at 25 Hz. In addition green outputs of up to 0.56 joules at 10 Hz have been produced.

The green output was again frequency doubled to 0.266 micron in ADP. Ultraviolet average powers of 1 watt (0.1 joule pulses at 10 Hz) were produced with a conversion efficiency of approximately 20%. Two problems with ADP prevented more efficient operation at high average powers: (1) the narrow half-width for temperature phase matching ($0.1^{\circ}C$) and (2) significant ultraviolet absorption, both linear and nonlinear (pump power dependent).

The ultraviolet output was used to pump an ADP parametric generator, degenerate at 0.53 micron and tunable throughout the visible spectrum. Performance of the generator was poor due to the problems in ADP mentioned above.

TABLE OF CONTENTS

LIST OF ILLUSTRATIONS

LIST OF ILLUSTRATIONS

Section I

INTRODUCTION

The purpose of this program was to experimentally investigate high average power second harmonic generation (SHG) and fourth harmonic generation (FHG) of Nd:$YAlO_3$ lasers (Nd:YAG was used on the program due to the nonavailability of Nd:$YAlO_3$ by the time the program started) and to investigate high average power optical parametric oscillation throughout the visible using the fourth harmonic of Nd:YAG as a pump.

A Nd:YAG oscillator (flash pumped and Q-switched) was followed by two Nd:YAG amplifiers to produce 1.06 micron output pulses in excess of one joule at repetition rates up to 25 Hz. This master-oscillator, power-amplifier (MOPA) system served as a pump source for SHG experiments. Deuterated cesium dihydrogen arsenate (CD*A) was used as the nonlinear material.

The 0.532 micron second harmonic was then used as the pump for the second SHG process from 0.532 micron to 0.266 micron, using ADP for the nonlinear material. The 0.266 micron output was then used as the pump for an ADP optical parametric generator (OPG) degenerate at 0.532 micron and tunable across the visible spectrum.

Among the achievements of this program are:

(1) Generation of 10 watts average power (0.4 joule pulses at 25 Hz) at 0.532 micron at a conversion efficiency of greater than 40%, without damage.

(2) Generation of 1 watt of average power (0.1 joule pulses at 10 Hz) at 0.266 micron, without damage.

(3) Identification of significant nonlinear absorption in ADP which drastically reduces its efficiency at high average powers.

It should be pointed out that the nonavailability of Nd:$YAlO_3$ had a serious impact on the program. First, the anticipated energy per pulse for the Nd:$YAlO_3$ system was greater than 2 joules, whereas the Nd:YAG system which

was actually used produced only a little over 1 joule. Secondly, the induced thermal birefringence of Nd:YAG at repetition rates above 10 Hz in our system caused severe depolarization of the laser beam, degrading the SHG conversion efficiency significantly. With Nd:$YAlO_3$, this problem does not exist, and the output beam is always linearly polarized. These two problems with Nd:YAG decreased the amount of useful 1.06 micron average power available as a pump for the SHG process by at least a factor of 2. Nevertheless, the program goal of 10 watts average power at 0.532 micron was obtained.

The physical properties of ADP (specifically nonlinear ultraviolet absorption) prevented the attainment of the program goal of 4 watts average power in the ultraviolet and in excess of one watt visible, tunable output. These problems are discussed specifically in Section IV and V. We did achieve 1 watt average power otuputs in the ultraviolet (0.1 joule pulses at 10 Hz) making this by far the highest power average power source in the ultraviolet below 3000Å demonstrated to date.

The remainder of this report is organized as follows. Section II contains a description of the Nd:YAG MOPA system, along with performance data. Section III describes SHG experiments in CD*A from 1.06 micron to 0.53 micron. Section IV describes FHG experiments from 0.532 micron to 0.266 micron in ADP. Section V describes visible parametric generator experiments in ADP. Section VI contains the summary and conclusions, and Section VII contains references to literature.

Section II

Nd:YAG LASER SYSTEM

2.1 GENERAL CONSIDERATIONS

Neodymium lasers are a natural choice for pump sources for nonlinear optical experiments for a number of reasons. These include their high efficiency, capability for high average power operation, and the availability of good quality, 90° phase-matchable crystals for SHG and FHG. The use of a MOPA system with $Nd:YAlO_3$ or Nd:YAG enables one to obtain Q-switched pulses with greater than one joule output at repetition rates up to a few tens of Hertz. Thus it was decided that a $Nd:YAlO_3$ or Nd:YAG MOPA system would be used as the pump source for this program. It was planned to build a second amplifier during the program for use with a Sylvania-owned oscillator and first amplifier, and the design goal was to produce 3 joule pulses at 30 Hz, using $Nd:YAlO_3$ laser rods. Unfortunately, by the time the program was begun, $Nd:YAlO_3$ was no longer available and Nd:YAG had to be used. The impact which this had on the program is discussed in subsection 2.2.

2.2 $Nd:YAlO_3$ vs Nd:YAG LASER SYSTEMS

It was originally proposed to use $Nd:YAlO_3$ as a laser material for this program for two basic reasons: (1) $Nd:YAlO_3$ has lower gain[1] than Nd:YAG, and hence can store more energy and (2) $Nd:YAlO_3$ provides linearly polarized outputs at all pump levels[2], whereas YAG's thermal birefringence substantially depolarizes the beam at high pumping levels[3]. The twofold advantage of higher energy per pulse and linear polarization make $Nd:YAlO_3$ a much better source for nonlinear optical applications, since both peak power and linear polarization are needed for nonlinear optical applications[4]. $Nd:YAlO_3$'s superiority over Nd:YAG as a pump for nonlinear optical applications had been demonstrated at the time the proposal for this program was submitted[5].

It was anticipated based on measured $Nd:YAlO_3$ data that a $Nd:YAlO_3$ MOPA system comprised of a 1/4" x 3" laser rod followed by a 1/4" x 3" first amplifier and a 3/8" x 3" second amplifier would provide in excess of two joule Q-switched pulses in a linearly polarized output beam. This system is illustrated schematically in Figure 2-1(a).

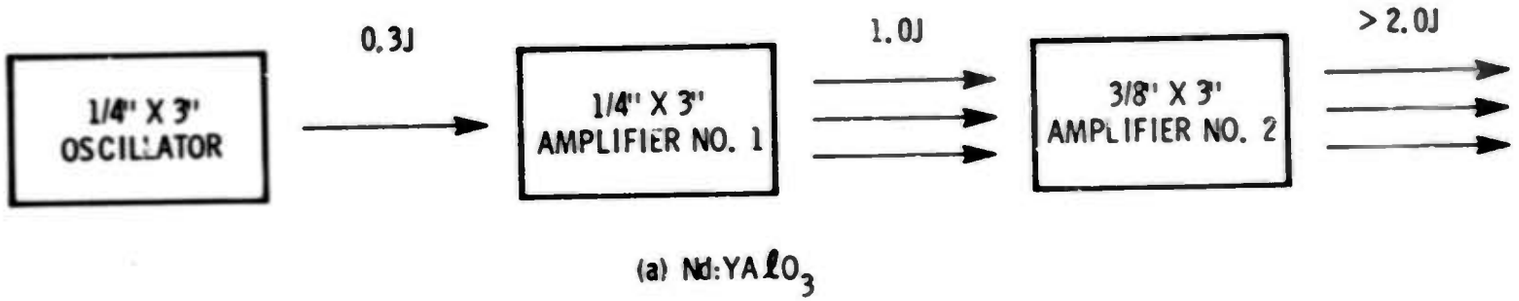

(a) Nd:YAlO$_3$

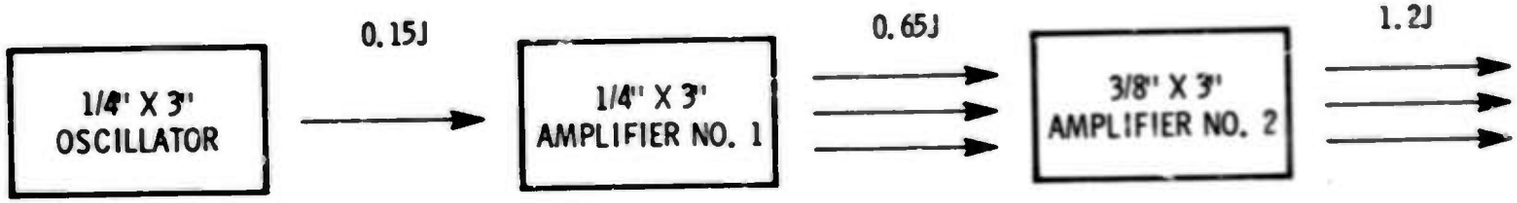

(b) Nd:YAG

Fig. 2-1 (a) Proposed Nd:YAlO$_3$ MOPA System, and (b) Actual Nd:YAG MOPA System

Unfortunately, by the time the program was begun, Nd:$YAlO_3$ was no longer commercially available, so that Nd:YAG had to be used. This had two important consequences for the laser system performance: (1) Nd:YAG will not store as much energy as Nd:$YAlO_3$, so that less energy per pulse was available (see subsection 2.5 for data) and (2) the thermal birefringence[3] of Nd:YAG at high pump levels substantially depolarizes the output beam (as much as 30% conversion to the orthogonal polarization). The combination of these two effects reduced the available useful 1.06 micron energy to less than half that anticipated from Nd:$YAlO_3$, thus reducing the average power obtainable at the second harmonic wavelength by at least a factor of 2 (barring saturation effects in the SHG process). The Nd:YAG system is illustrated in Figure 2-1(b).

2.3 LASER SYSTEM DESIGN CONSIDERATIONS

In this section we will briefly discuss some of the design considerations for the Nd:YAG MOPA system which was built up for use on this program, including choice of Q-switches, pump cavities and geometries, choice of TEM_{oo} or multimode operation, and other similar considerations.

2.3.1 Q-Switch Selection

Nd:YAG lasers can be conveniently Q-switched in two ways: (1) a rotating mirror, and (2) electro-otpically. In general, rotating mirror Q-switching provides more efficient operation and greater energy outputs, while electro-optic Q-switching is much more convenient and reliable. It was decided to fabricate a rotating mirror Q-switch for use on this program. This Q-switch is driven by an air turbine and can be spun up to 50,000 RPM and is shown in the photograph in Figure 2-2. The Q-switch is basically a rotating prism, which is placed in front of a mirror to optically double the rotation rate.

An electro-optic Q-switch was also used on the program. This Q-switch is a longitudinal KD*P crystal (c-axis), with electrodes on the end faces. A photograph of this Q-switch is shown in Figure 2-3.

In general, we obtained much better conversion efficiency using the electro-optic Q-switch, even though the laser system had about the same 1.06 micron otuput with either Q-switch. These experiments are discussed in Section 2.5.

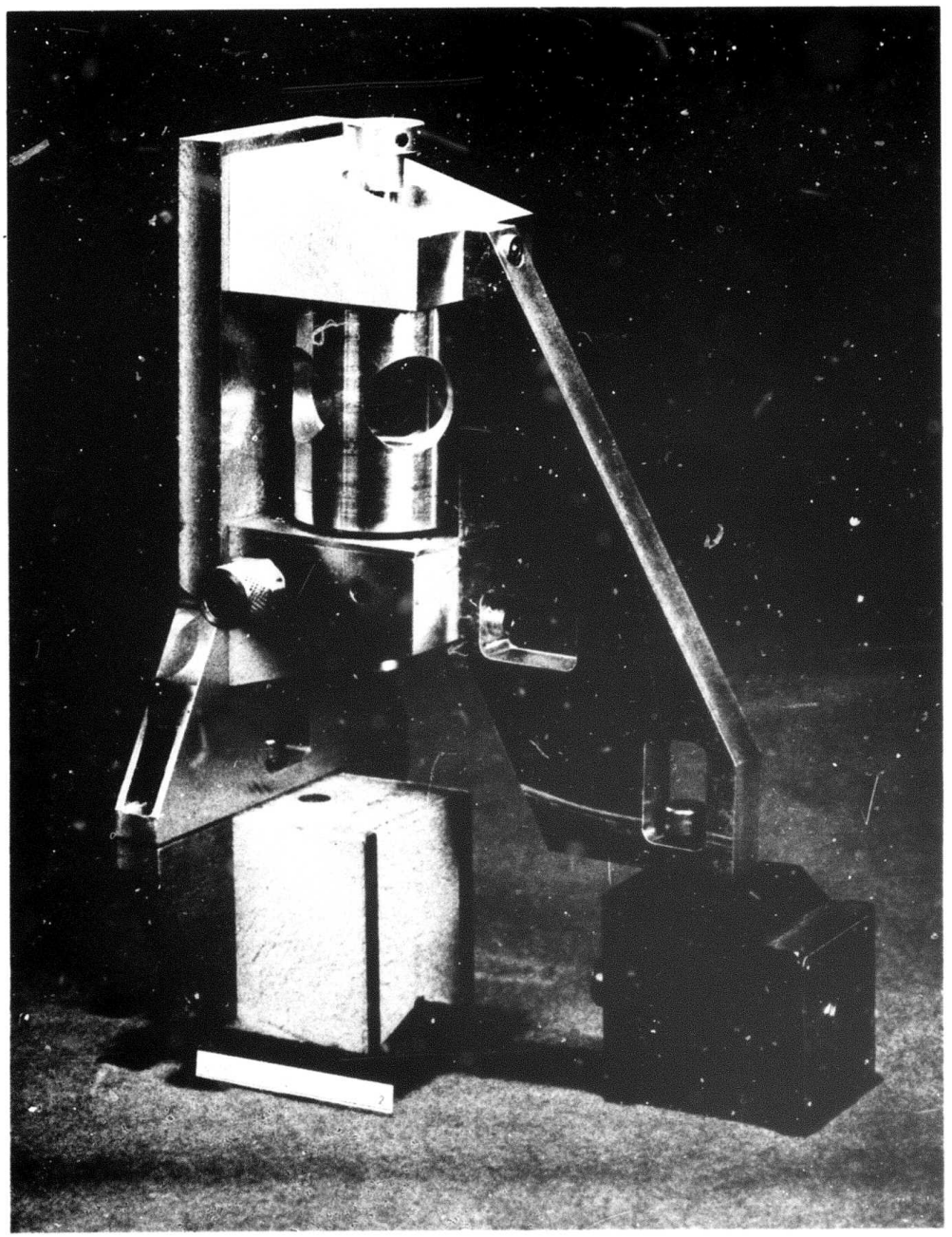

Fig. 2-2 Rotating-prism Q-switch used on program

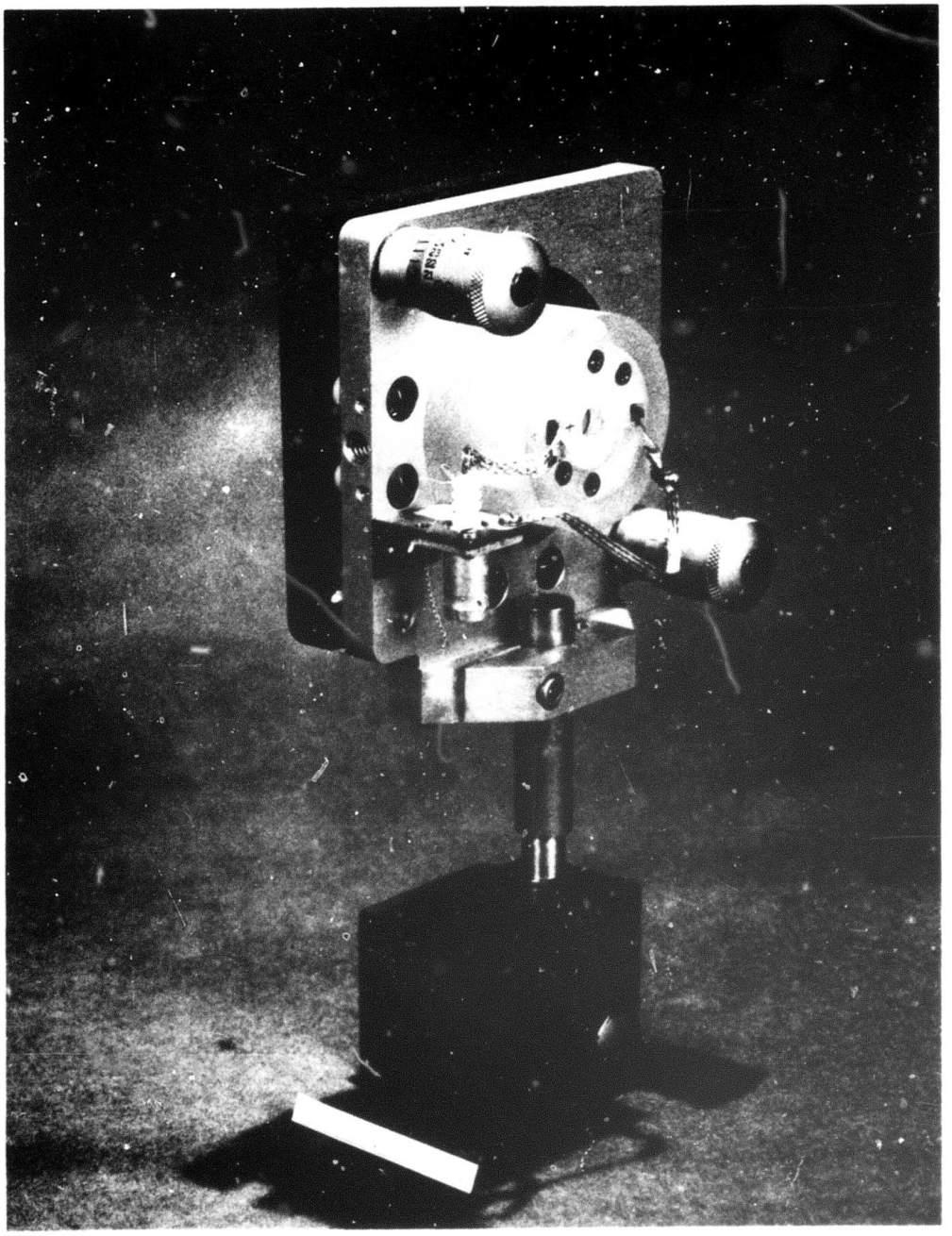

Fig. 2-3 Electro-optic Q-switch used on program

2.3.2 Choice of Pump Cavities, Geometry, and Flashlamps

In order to obtain most efficient laser operation with good mode control, we investigated the use of both silver and gold reflecting coatings on the pump cavities, different pumping geometries, and both Kr and Xe lamps.

Figure 2-4 shows the normal mode oscillator output with Krypton lamps and with gold or silver coatings on the pump cavity. Since the gold coating gives better performance and is more durable, it was used.

Figure 2-5 shows a comparison of Krypton and Xenon lamps. Since the two gave approximately the same output, it was decided to use Xe lamps because of their longer lifetime.

In Figure 2-6 is shown a comparison of 5 mm bore and 3 mm bore lamps. In our laser head, the larger bore lamps gave higher outputs, so they were used.

Figure 2-7 shows a comparison of elliptical inserts of various eccentricities. One ellipse is a 45° ellipse (which we term "elliptical") and the other is an 80° ellipse (almost round, so we term it "round"). Since the outputs are almost identical and since the round cavity gives a much more spatially uniform output, the round cavity was employed.

2.3.3 Laser Head Design

A photograph of a disassembled laser head is shown in Figure 2-8. The laser head is flooded with flowing tap water for cooling. A nonex glass tube surrounds the laser rod to shield it from ultraviolet radiation from the flashlamps. The laser head employs a single pump lamp, as shown, and the pump cavity inserts can be changed. A 1/4" x 3" Nd:YAG rod is used, and its ends are parallel and wedged 5°. The oscillator and first amplifier heads are identical. The ends of the Nd:YAG rods protrude from the ends of the laser head for easy cleaning and to prevent metal vapor from being deposited on the rod ends due to stray laser light vaporizing metal from flow tubes.

Figure 2-9 shows a photograph of the second amplifier head, which employs two flashlamps in a double-elliptical pump cavity, and uses a 3/8" x 3" rod with parallel ends wedged 5°. It is also flooded with flowing tap

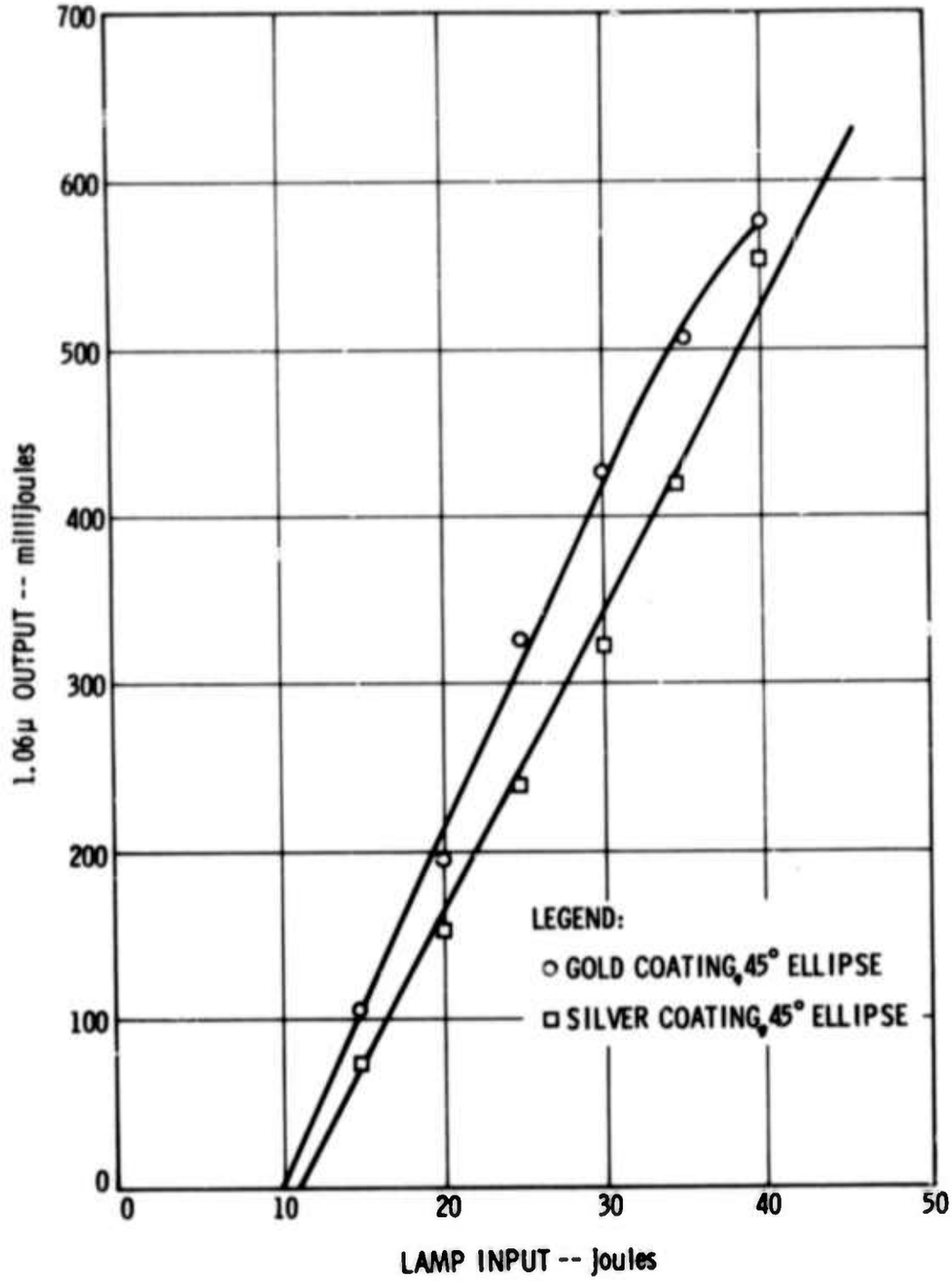

Fig. 2-4 Comparison of Laser Oscillator Performance with Gold and Silver Coatings on the Laser Pump Cavity

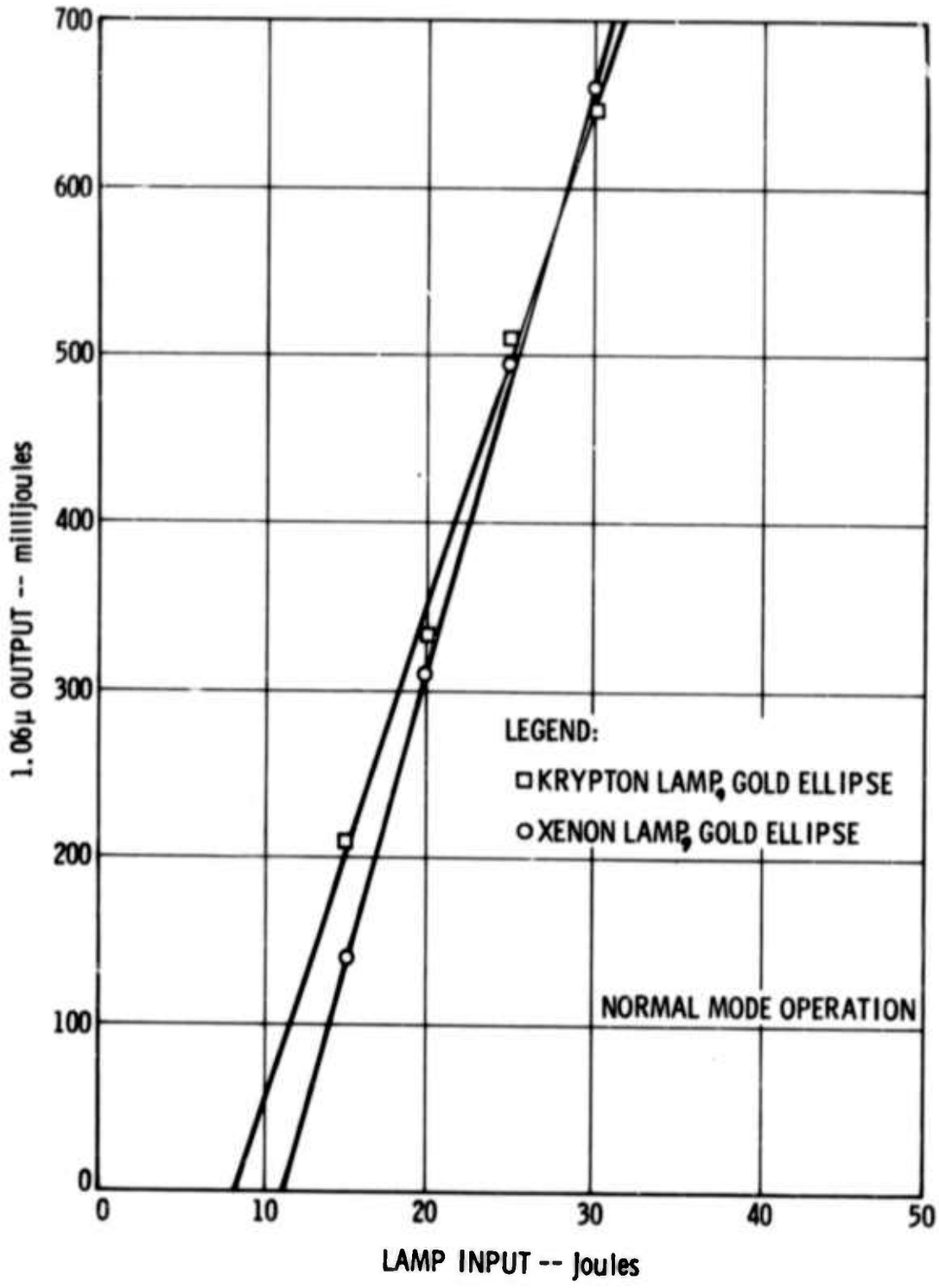

Fig. 2-5 Comparison of Pumping Efficiency of Krypton and Xenon Lamps

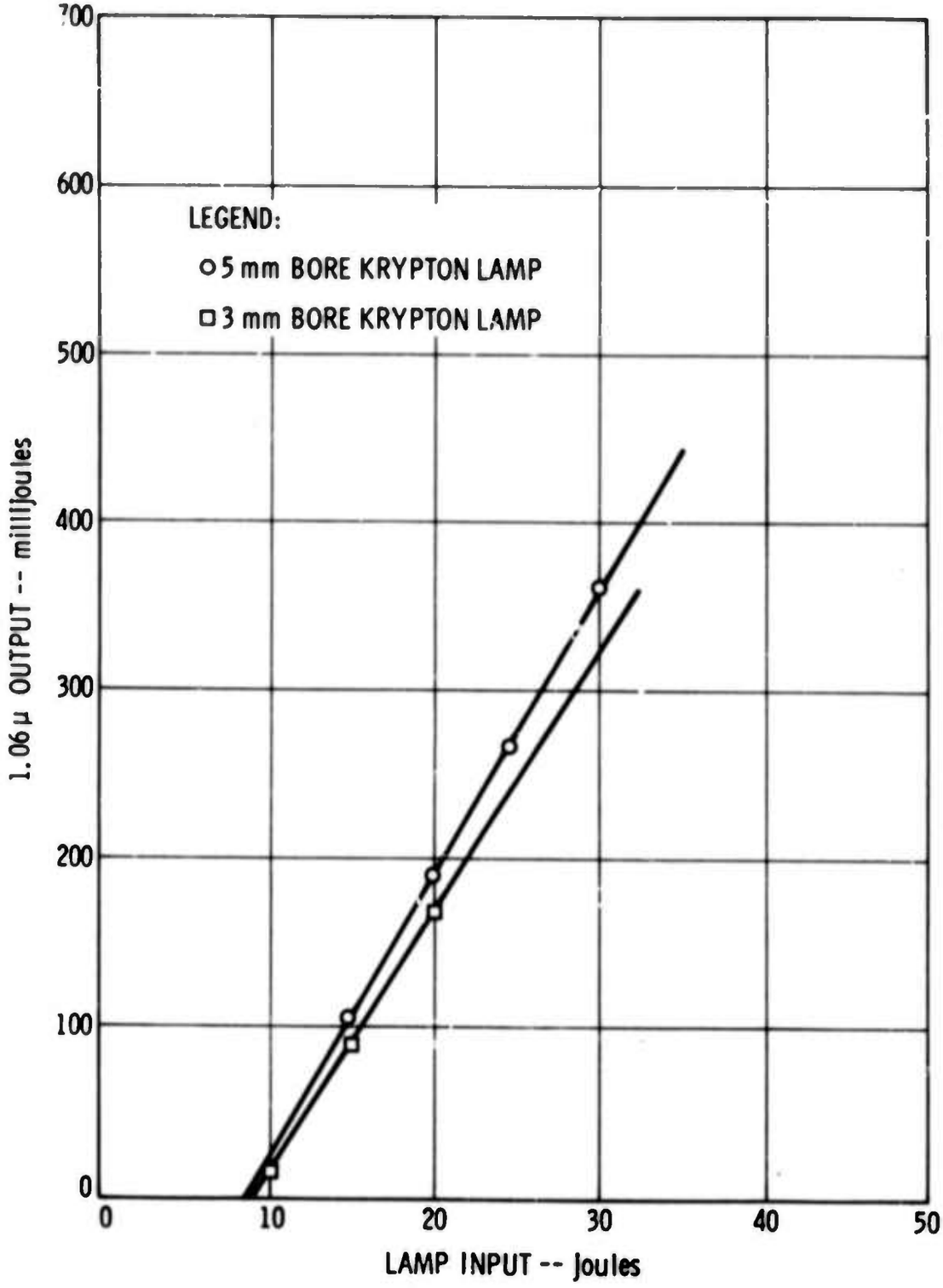

Fig. 2-6 Comparison of Pumping Efficiency of 3 mm and 5 mm Diameter Bore Lamps

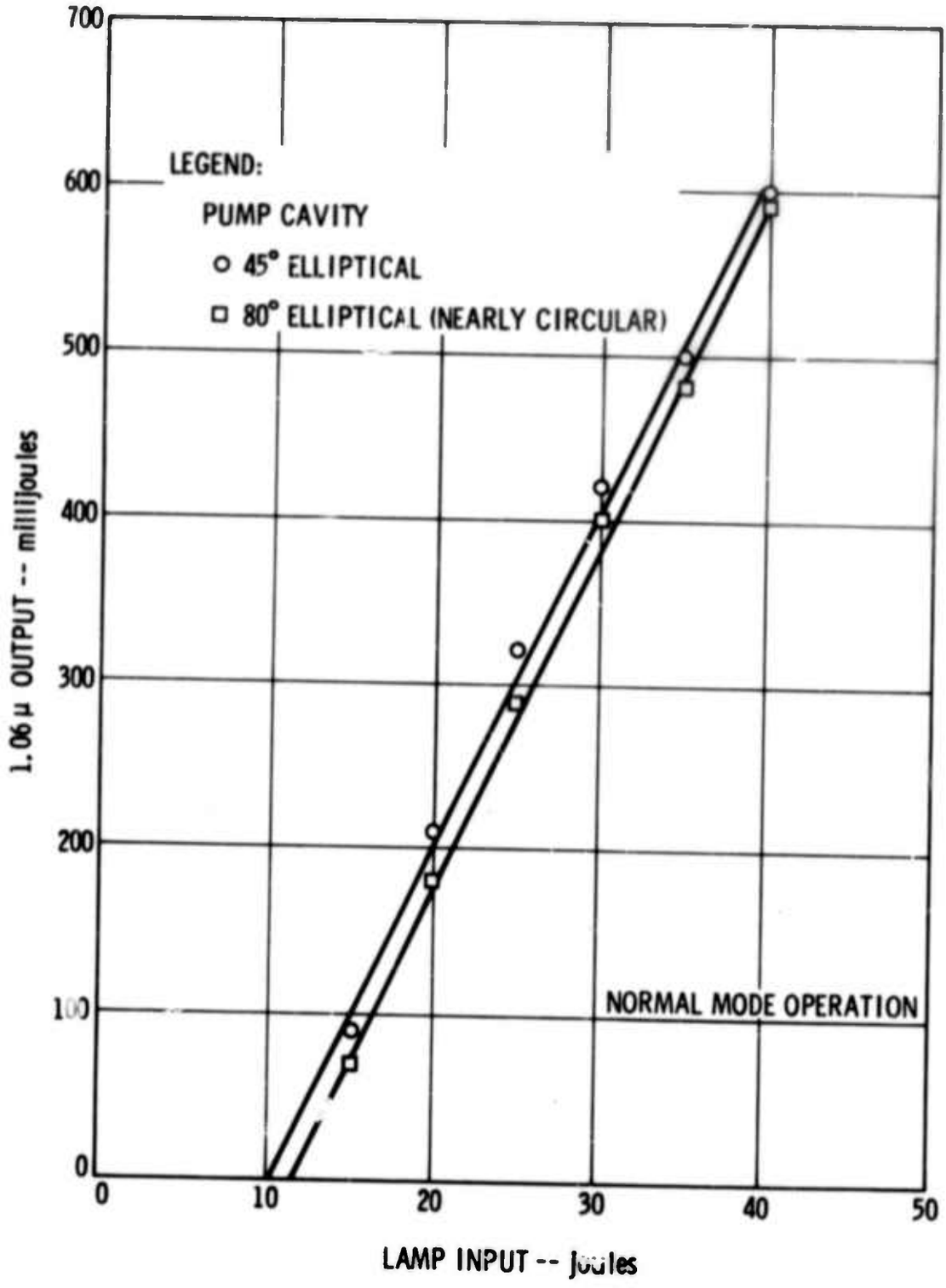

Fig. 2-7 Comparison of Pumping Efficiency of Elliptical Inserts of Different Eccentricities

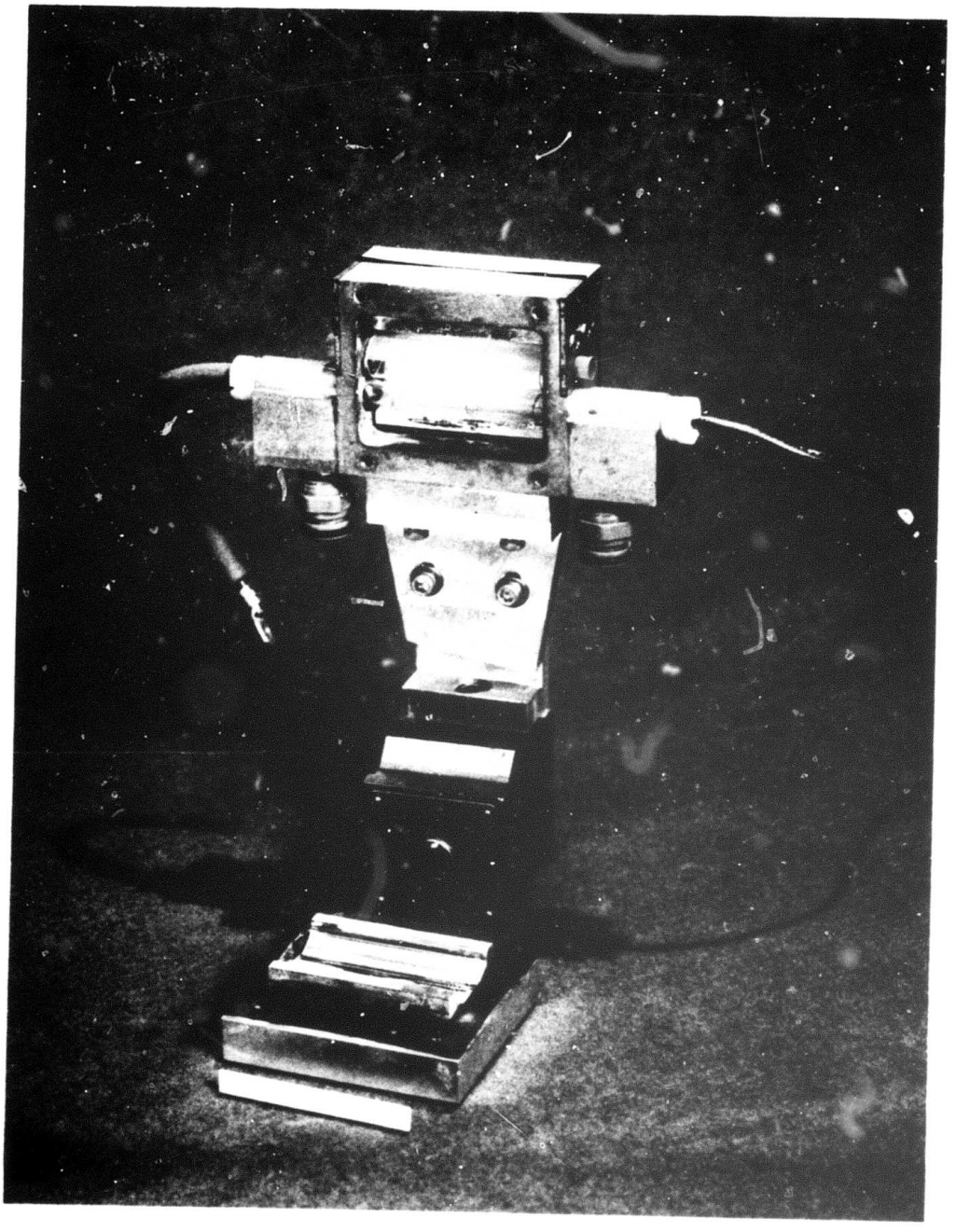

Fig. 2-8 Laser head design used for oscillator and first amplifier

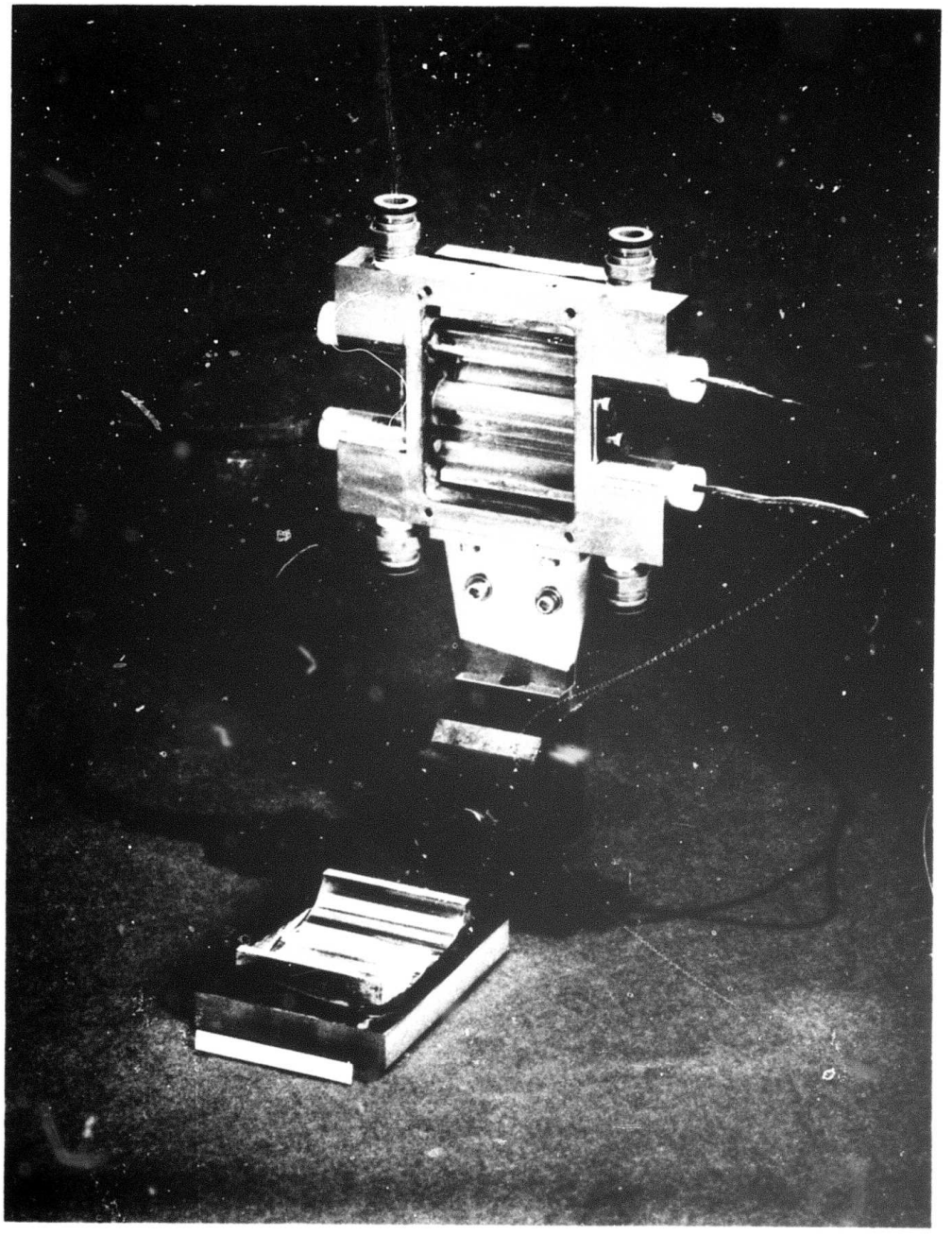

Fig. 2-9 Laser head design used for second amplifier

water for cooling, and has replacable cavity inserts. Provision was made in all three heads to insert samarium glass filters to limit superadiance.

2.3.4 TEM_{oo} vs Multimode Operation and Polarized vs Unpolarized Operation

Ideally, one would like a TEM_{oo}, linearly polarized pump source for nonlinear optical applications. In practice, this is not always necessary. Since all of the nonlinear crystals used on this program are 90^{o} phase matchable, they have large angular acceptance angles and can phasematch multimode beams which have larger divergences than TEM_{oo} beams. Another possible problem with multimode beams is hot-spots, which may cause damage to laser rods or nonlinear crystals. It was found experimentally, however, that damage did not occur, and that efficient conversion could be obtained with multimode beams. Because of this, and because multimode systems are much more efficient than TEM_{oo} systems, the oscillator was operated in a high order transverse mode. This configuration also gives higher output pulse energies.

The SHG process requires a linearly polarized pump beam, so that in general one would like a linearly polarized output beam from the laser. However, all crystals have some absorption which limits the maximum average power that a single crystal can efficiently convert to the second harmonic. In this case it becomes necessary to use more than one crystal. If this is the case, two arrangements are possible: (1) both crystals can be oriented the same way, requiring the same beam polarization (the crystals can be either in series or parallel) or (2) the crystals can be rotated 90^{o} with respect to each other, requiring orthogonal beam polarizations (again the crystals can be in series or in parallel). In the latter case, the pump beam can be unpolarized. Running the laser in the unpolarized configuration has a definite advantage, namely that at high pumping rates the thermal birefringence of Nd:YAG has no effect. The laser can be operated unpolarized by using the rotating mirror Q-switch. For these reasons, we anticipated that better performance would be obtained with the rotating mirror Q-switch than with the electro optic Q-switch. In fact, however, we obtained better SHG with the electro-optic Q-switch, as described in Section 2.5.

2.4 LASER SYSTEM CONFIGURATION

In this section we will discuss the actual MOPA configuration used in the SHG experiments. A schematic of the entire system is shown in Figure 2-10 for the case of electro-optic Q-switching. For rotating mirror Q-switching, timing was derived from the rotating prism rather than the rate generator.

As mentioned previously, all laser heads were water cooled. Provision was made for closed cycle cooling so that the water temperature could be raised to reduce the gain of the Nd:YAG rods and hence increase their energy storage.

All flashlamps are series triggered, and each lamp is driven by a separate power supply. The maximum repetition rate is limited by the maximum average power rating of the power supplies of 1.5 KW.

Figure 2-11 shows a photograph of the entire MOPA assembly, including oscillator, amplifier #1, and amplifier #2. Beam expansion is provided by propagation. The beam is folded using two TIR prisms as shown. All components are mounted on magnetic bases which are clamped to a steel table top.

Figure 2-12 shows a photograph of the charging power supplies (console #1), the control console (console #2), the capacitor storage bank (console #3), and the heat exchanger system.

2.5 LASER SYSTEM PERFORMANCE

2.5.1 Basic Laser Operating Characteristics

Figure 2-13 shows the Q-switched output of the oscillator using the rotating prism Q-switch. The oscillator saturates at $\sim$ 260 mJ due to superradiance. In order to try to increase the Q-switched output, a piece of somarium glass was inserted in the cavity to suppress superradiance, but no improvement was found, as indicated in the figure.

Figure 2-14 shows the effects of Q-switch rotation rate. No further improvement was found by increasing the rotation rate beyond 800 Hz, so the Q-switch was operated at this rate for the remaining experiments.

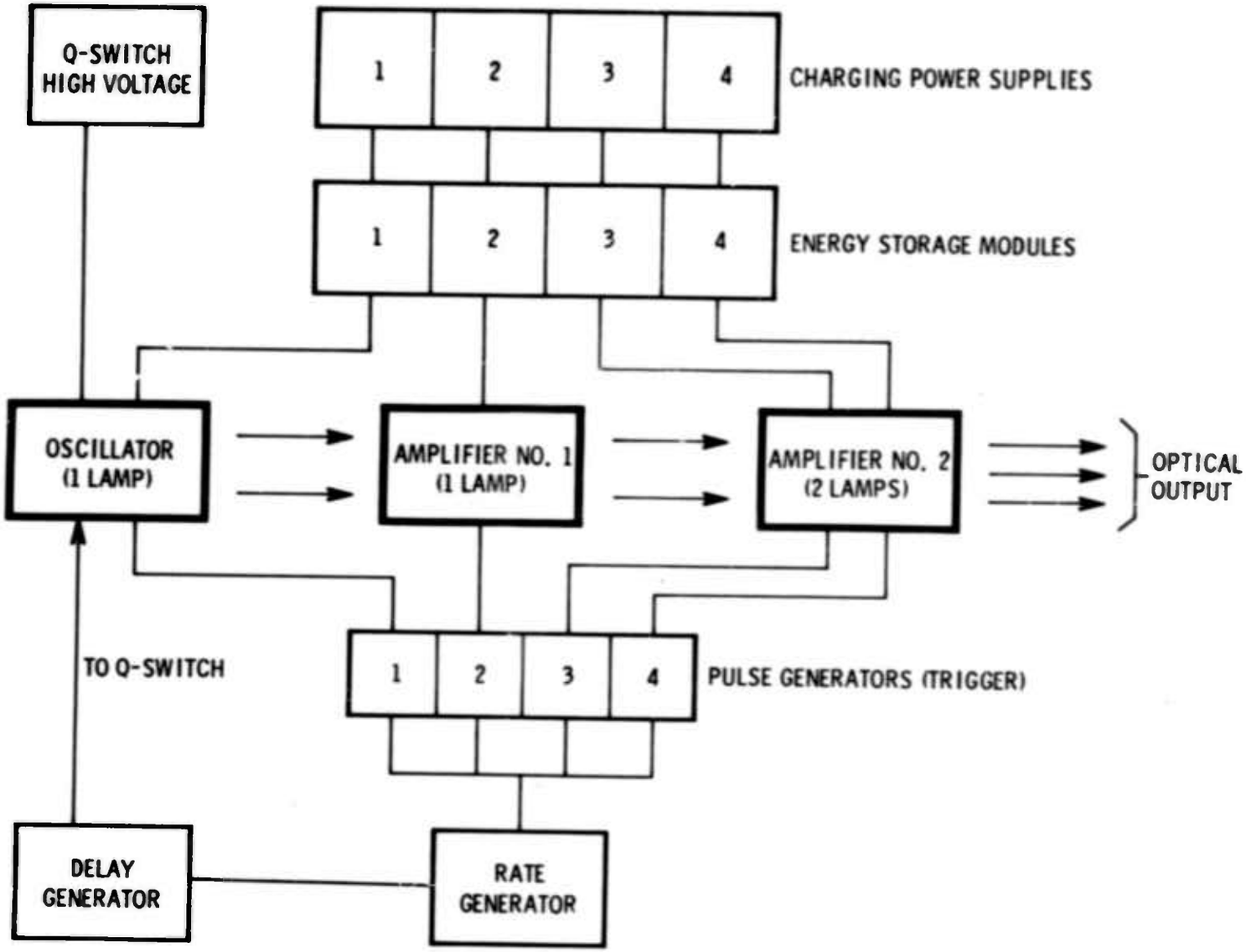

Fig. 2-10 Schematic of Nd:YAG MOPA System

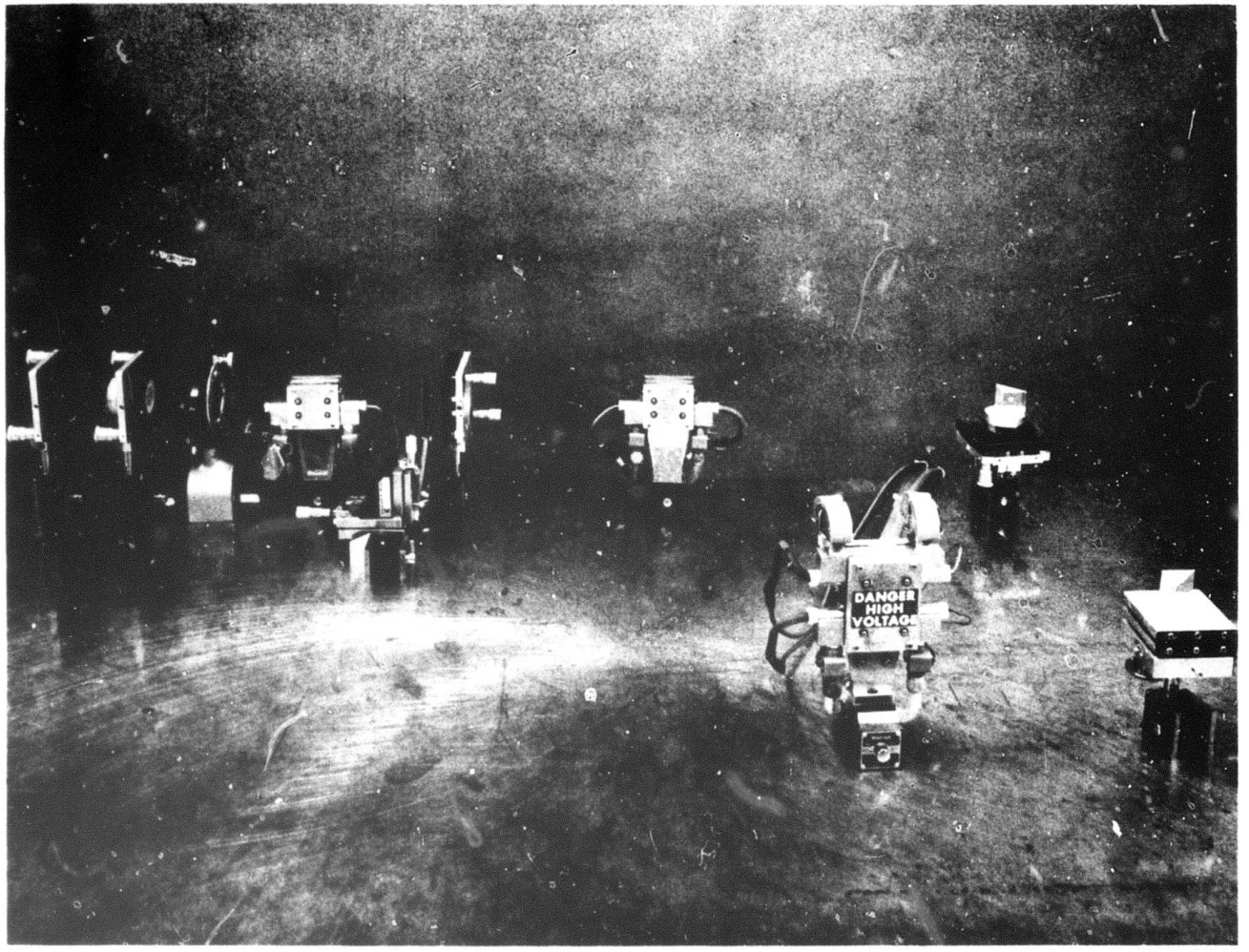

Fig. 2-11 Photograph of MOPA system showing the Q-switched oscillator, amplifier #1, and amplifier #2.

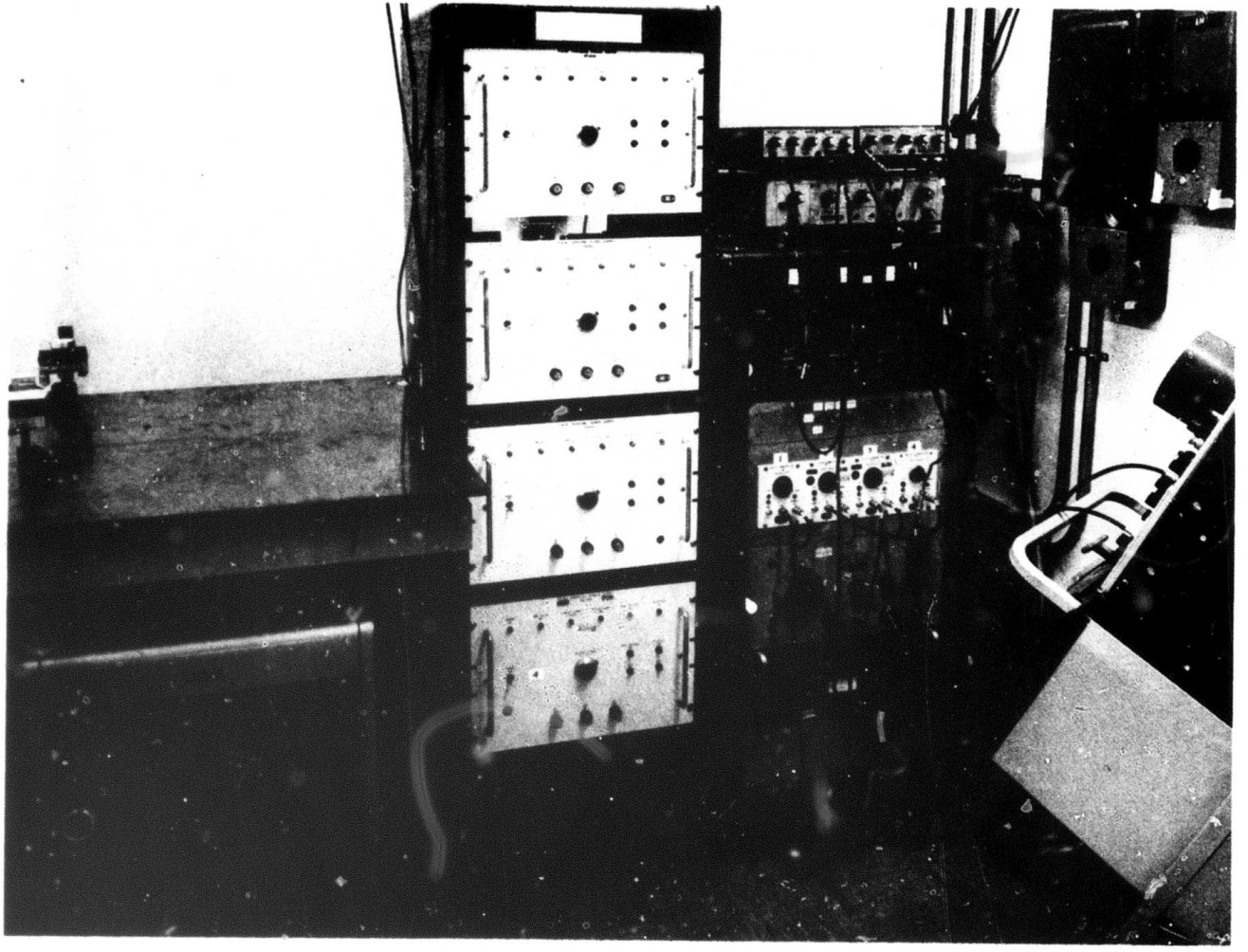

Fig. 2-12 Photograph of the charging power supplies, the control console, and the capacitor storage bank.

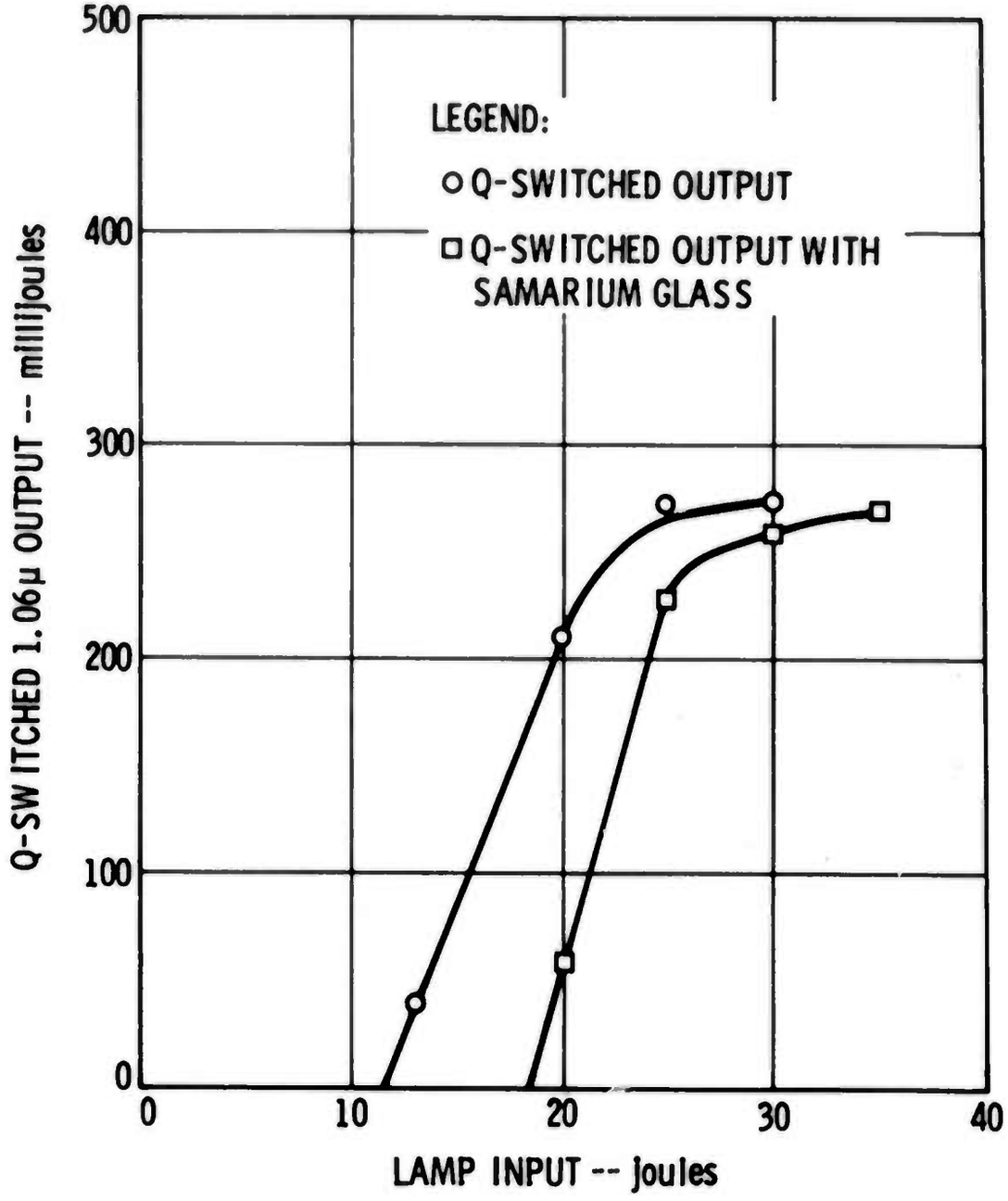

Fig. 2-13 Q-Switched Output of Nd:YAG Oscillator. Results are Shown with and without Samarium Glass.

Figure 2-15 shows the Q-switched output from the oscillator using the electro-optic Q-switch. The output is considerably less than with the rotating mirror, but, as we will see later, the output from the entire MOPA system is about the same with either Q-switch.

Figure 2-16 shows the performance of the first amplifier as a function of input pump (electrical) energy for various oscillator levels. The amplifier begins to saturate at the 40 joule level, giving $\sim$ 1/2 joule extracted at 1.06 micron. Increasing the cooling water temperature to $\sim$ 85°C in both oscillator and amplifier increased the output by $\sim$ 10%, but the added complexity discouraged running the system at elevated temperatures.

Figure 2-17 shows the output from the second amplifier as a function of pump energy, for various optical inputs. The maximum output obtained was 1.25 joules. All data were obtained at 10 Hz.

When the rotating prism was replaced by an electro-optic Q-switch, the oscillator output dropped to $\sim$ 150 mJ, and the output from the whole system was reduced to $\sim$ 1.1 joules, but the output beam was much cleaner. In addition, the pulselength was reduced from $\sim$ 30 nsec to $\sim$ 12 nsec, providing much higher peak powers.

2.5.2 Depolarization and Other Deleterious Effects

In order to determine to what extent depolarization of the laser beam would occur with higher repetition rates, the polarization in the parallel and perpendicular directions was measured at the output of the laser. This data is shown in Figure 2-18. The laser was internally polarized with a Brewster plate, and the relative powers in the parallel and perpendicular polarizations were measured as a function of repetition rate. It is evident that the laser is severely depolarized at high repetition rates. A better polarizer would eliminate much of this fall-off, but if a polarizer is used, one might just as well use an electro-optic Q-switch.

Figure 2-19 shows the single pass depolarization of the first amplifier for a well polarized input as a function of repetition rate. Again, substantial beam depolarization results; with the use of Nd:$YAlO_3$ of course, there would be no beam depolarization.

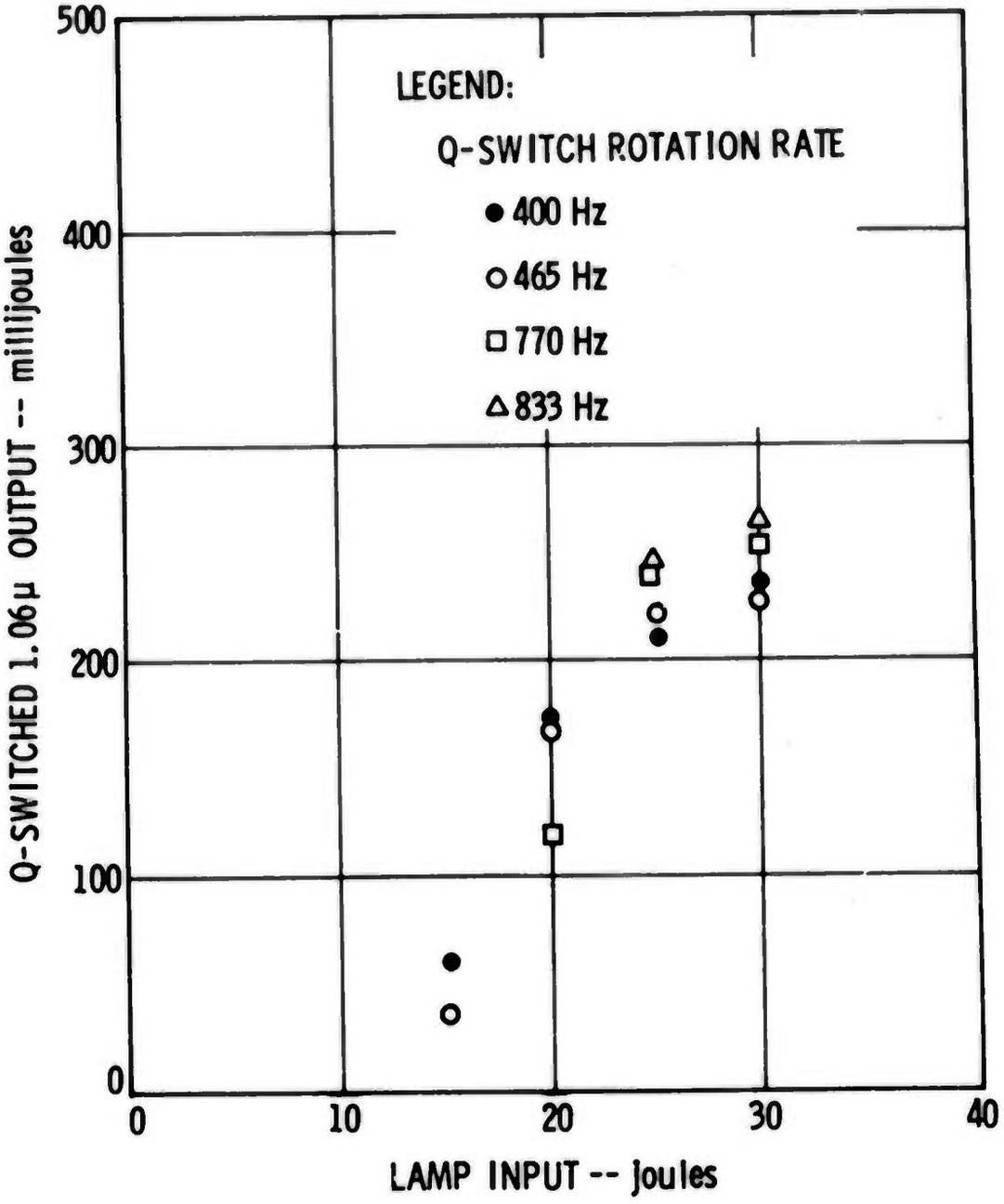

Fig. 2-14 Laser Output Versus Q-switch Rotation Rate

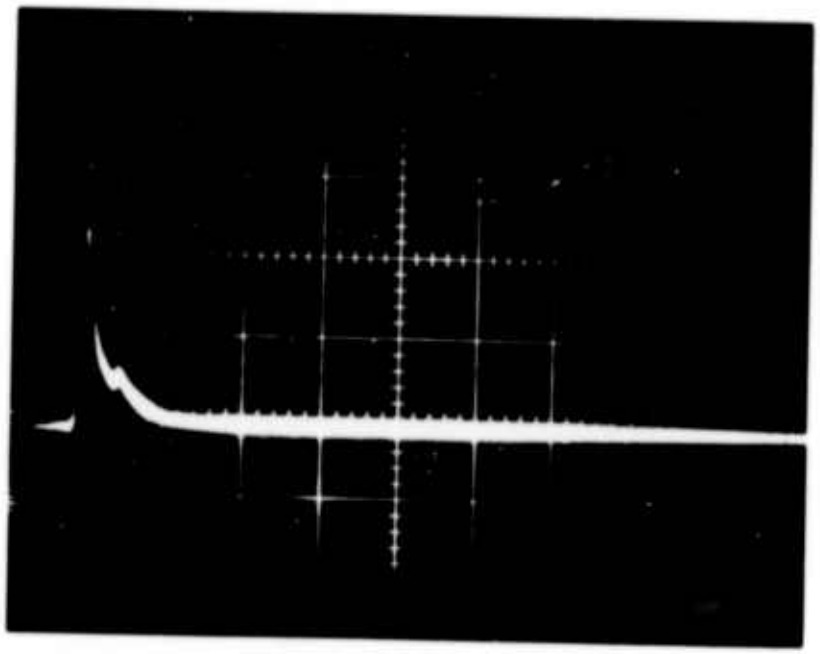

Fig. 2-15 Q-switched Pulse Obtained Using Electro-Optic Q-switch. Scale is 100 ns/division.

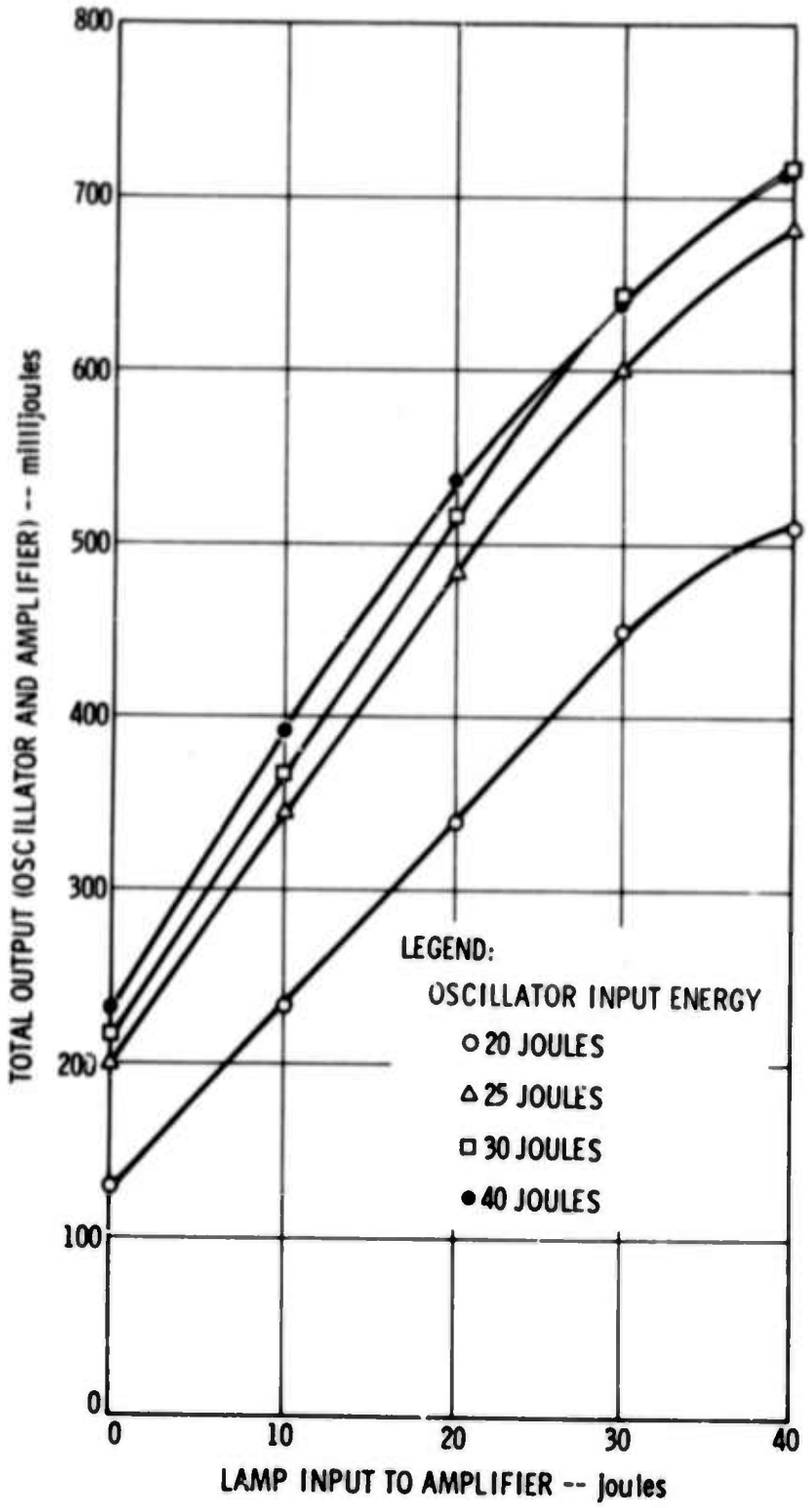

Fig. 2-16 Output from First Amplifier Versus Input Energy

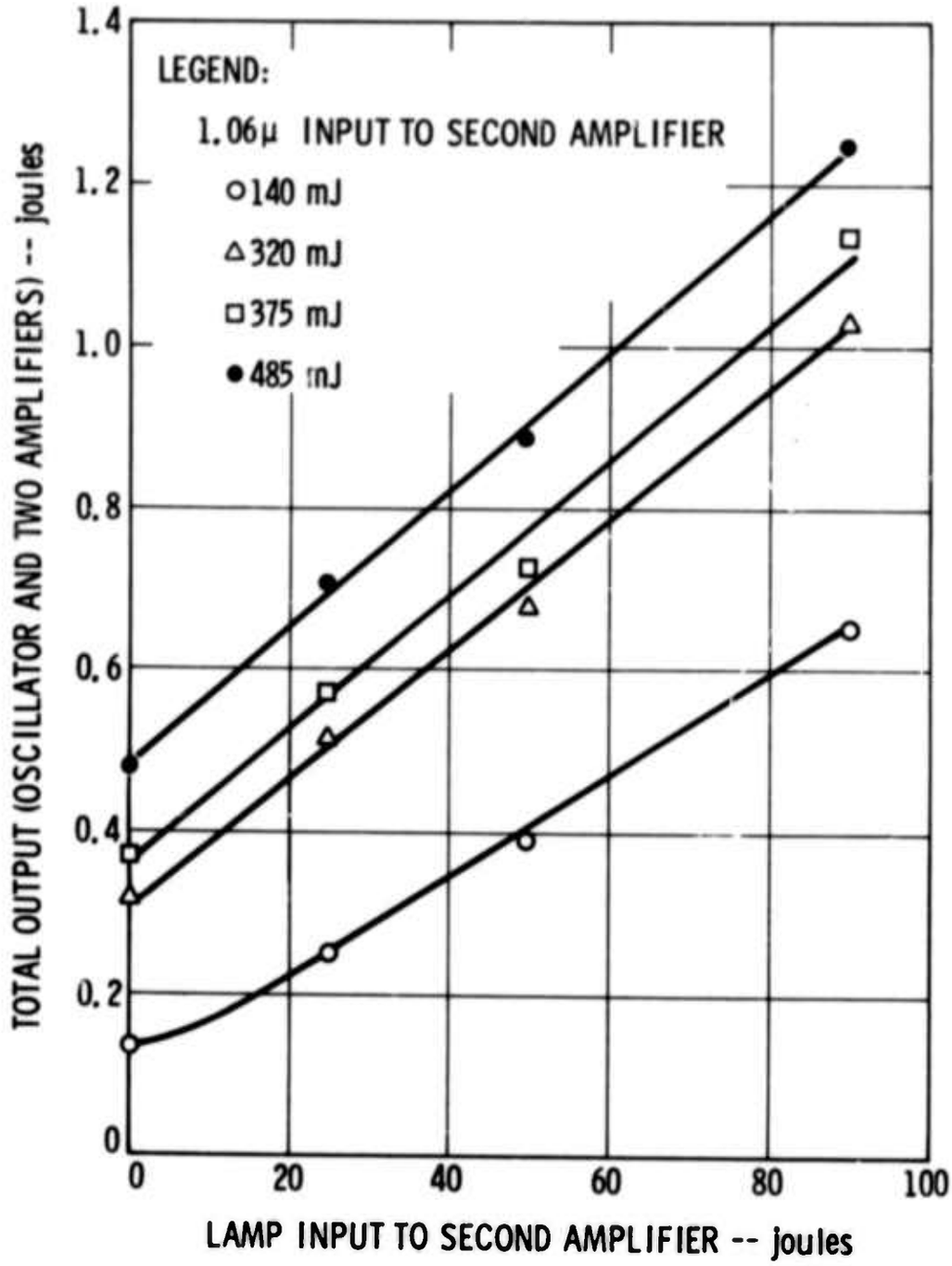

Fig. 2-17 Output from Second Amplifier Versus Input Energy

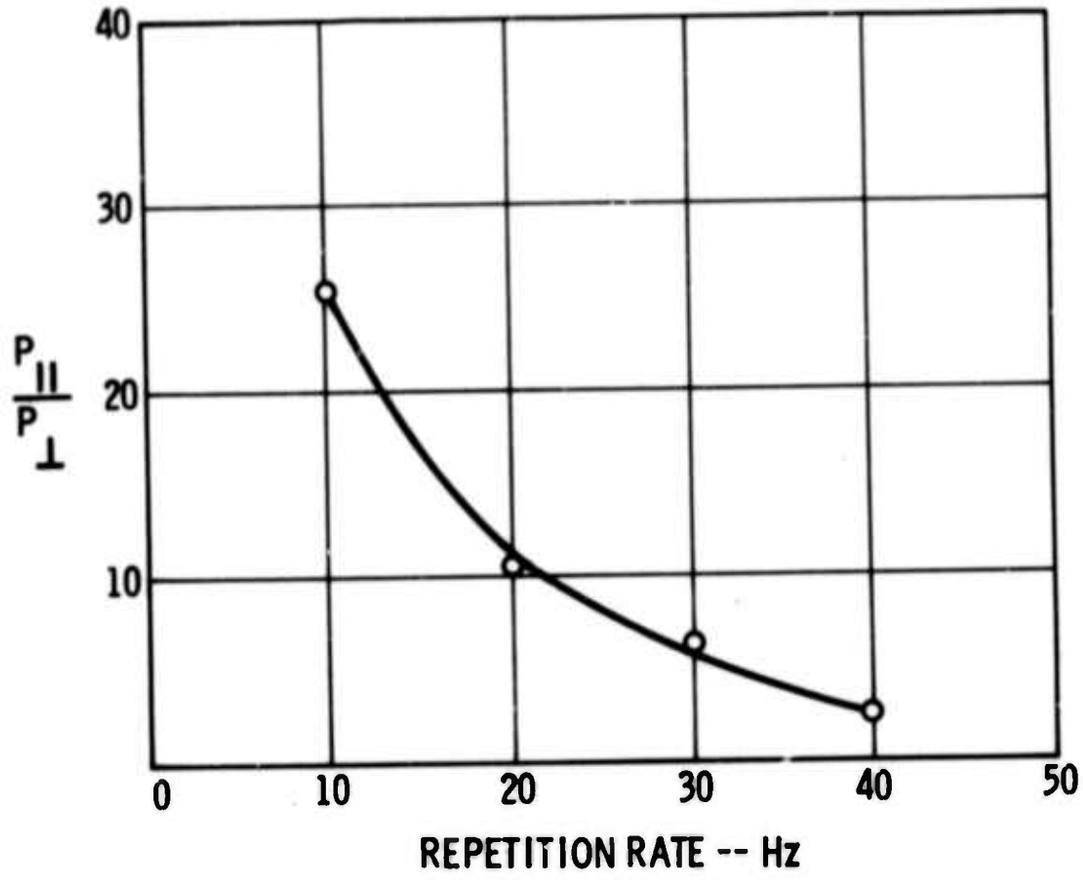

Fig. 2-18 Polarization Properties of the Laser Oscillator Versus Repetition Rate

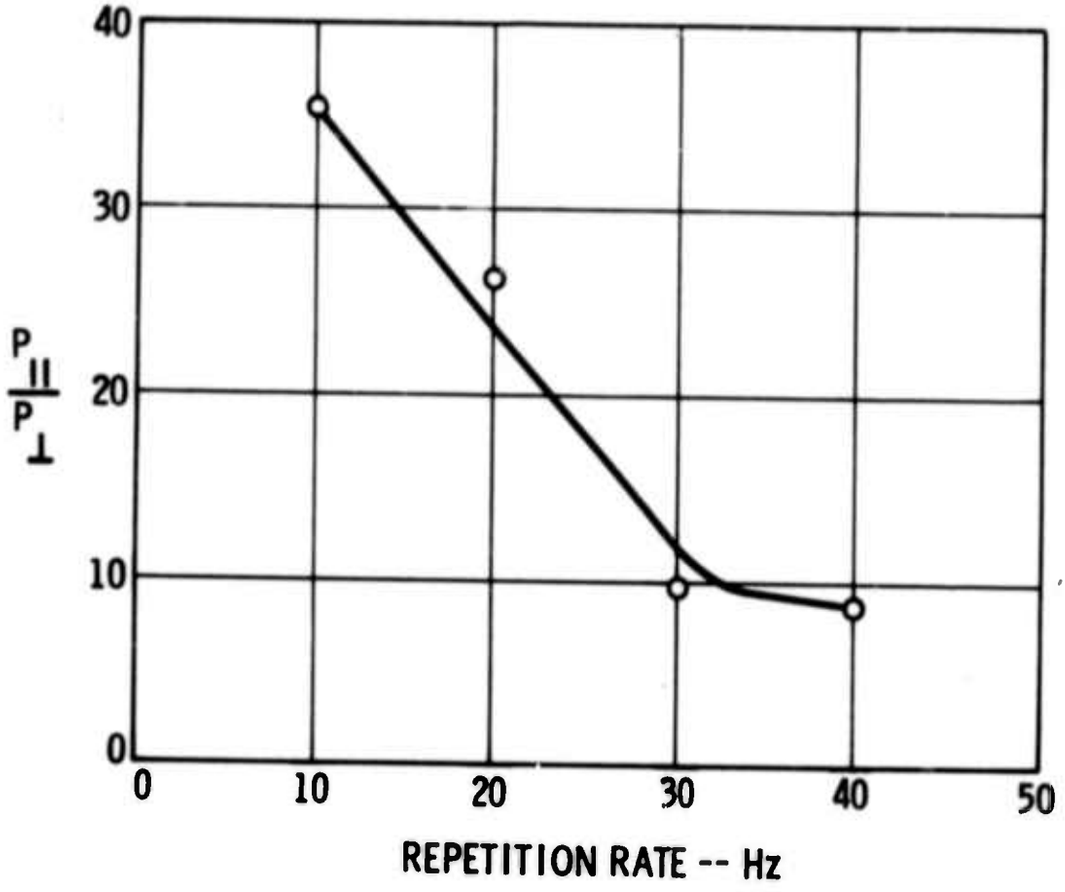

Fig. 2-19 Depolarization of the First Amplifier Versus Repetition Rate

Section III

SECOND HARMONIC GENERATION FROM 1.06 MICRON TO 0.532 MICRON

3.1 CESIUM DIDEUTERIUM ARSENATE (CD*A)

Our previous experience with various nonlinear crystals indicated that CD*A is the best available nonlinear crystal for frequency doubling multimode, high peak power 1.06 micron lasers. It is 90° phasematchable at 103°C, with a temperature halfwidth of ∿ 5°C for a 1 cm crystal. Thus four 12 mm x 12 mm x 20 mm CD*A crystals were ordered from Quantum Technology, Ltd. of Canada, which is presently the only commercial supplier of CD*A.

A transmission curve for one of the crystals is shown in Figure 3-1. The crystal is nominally transparent at both the fundamental wavelength at 1.0648 micron and the second harmonic at 0.532 micron. The crystals were of good optical quality, except for numerous small cleaves on the surface which ran parallel to the length.

The CD*A crystals were held in a temperature controlled oven, which could be adjusted in position and tilt. One of those oven assemblies is shown in Figure 3-2.

The unfocused 3/8" diameter output beam from the laser system was directed onto the uncoated CD*A crystal, which was heated to slightly below the phase matching temperature. When the laser was turned on, the crystal angle was adjusted slightly to achieve phase matching. As the crystal heated slightly due to absorbed 1.06 micron light, the angle was correspondingly adjusted to maintain phase matching.

3.2 SHG RESULTS WITH CD*A

3.2.1 Experiments with Rotating Prism Q-Switching

Initial experiments were performed at 10 Hz. With an input 1.06 micron energy of ∿ 1.2 joules/pulse, the green output energy was ∿ 0.25 joules, giving a conversion efficiency of ∿ 20%. The output energy was determined by using a CRL power meter with a calibrated diffuser in front of it and dividing the average power by 10 to determine the pulse energy. This same method was used to measure the 1.06 micron power.

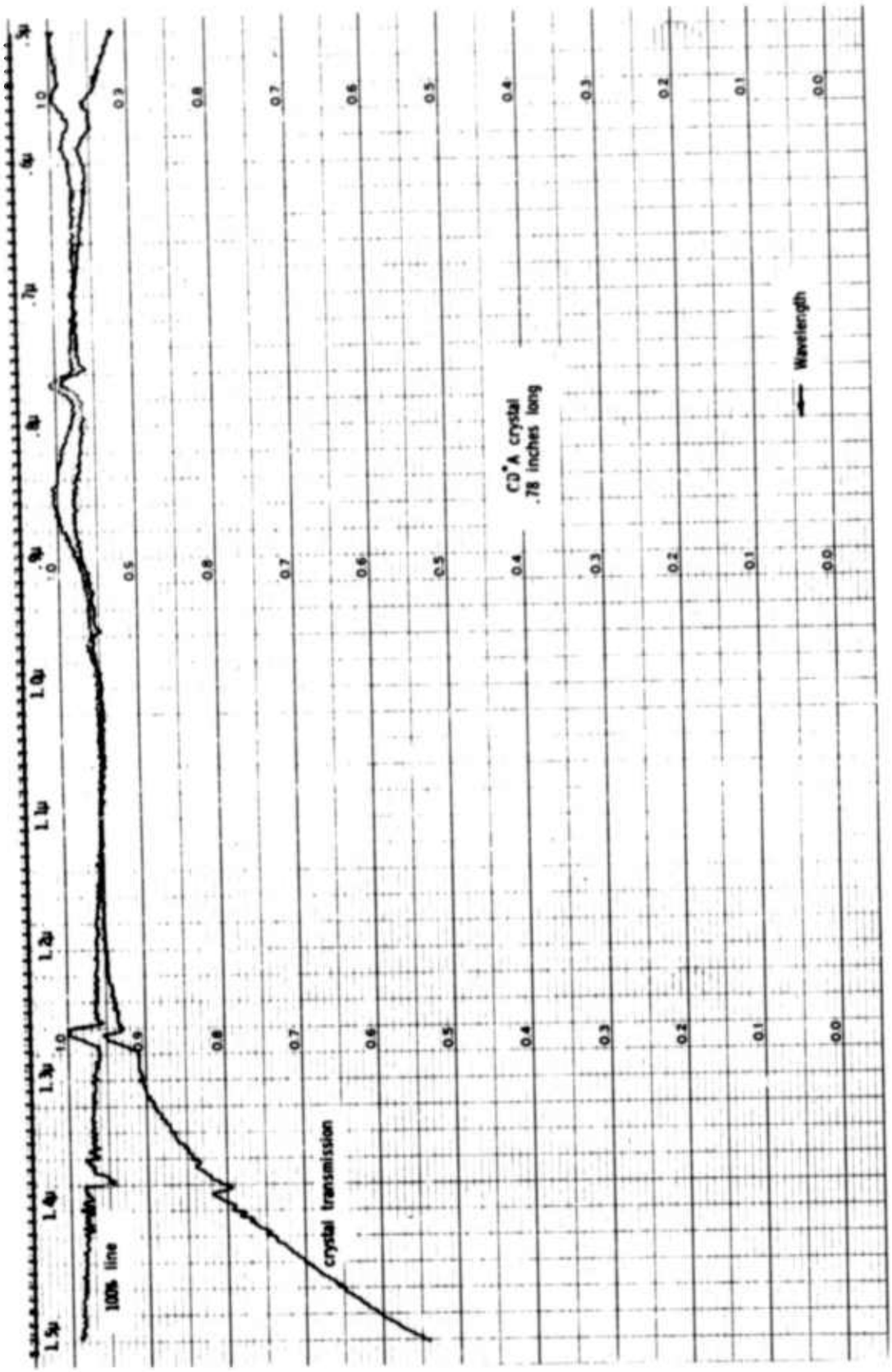

Fig. 3-1 Spectral Transmission of 2 cm Long CD*A Crystal

Fig. 3-2 Oven assembly

Figure 3-3 shows the green output power as a function of repetition rate, using the rotating prism. The green power saturates badly with increasing repetition rate. This is due to two laser effects, not saturation of the CD*A crystal. One reason for the fall off is depolarization of the oscillator with increasing repetition rate as shown in the section 2.5.2. To verify this, we performed SHG experiments with the oscillator alone, thus giving much lower average powers, and found the same saturation. The other effect which contributes to the fall off is lengthening of the 1.06 micron pulse with increasing repetition rate, as shown in Figure 3-4, which shows the 1.06 micron pulselength at 10, 20, 30, and 40 Hz. Note that the peak power decreases and the pulselength increases as the repetition rate is increased.

In an attempt to compensate for the depolarization of the laser, we performed an experiment using two CD*A crystals rotated 90° with respect to each other, so that one crystal would frequency double each laser polarization. Unfortunately, the laser depolarization was not complete, so that one crystal had only 50% as much 1.06 micron power density as the other. Since the SHG conversion depends on the square of the pump power, only 25% as much green was produced by this crystal. This increase was offset by reflection losses from using two crystals rather than one.

In order to increase the conversion efficiency at 10 Hz beyond the 20% obtained with an unfocused beam, a lens was used to focus the output into the CD*A doubler crystal. At a conversion efficiency of $\sim$ 25%, slight crystal damage occurred, so further focusing was not attempted.

It should be mentioned at this point that the output beam distribution from the MOPA system with the rotating prism Q-switch was very poor, containing many hot-spots. In addition the beam was much more intense on one side due to the rotation of the Q-switch. For these reasons, it was decided to try the electro-optic Q-switch in the oscillator. SHG experiments using the electro-optically Q-switched system are described in the next section.

3.2.2 Experiments with Electro-Optic Q-Switching

When the oscillator is Q-switched electro-optically, its output is reduced to about 140 mJ. However, the beam is much more uniform. At the output of the second amplifier, the energy is about the same as with the

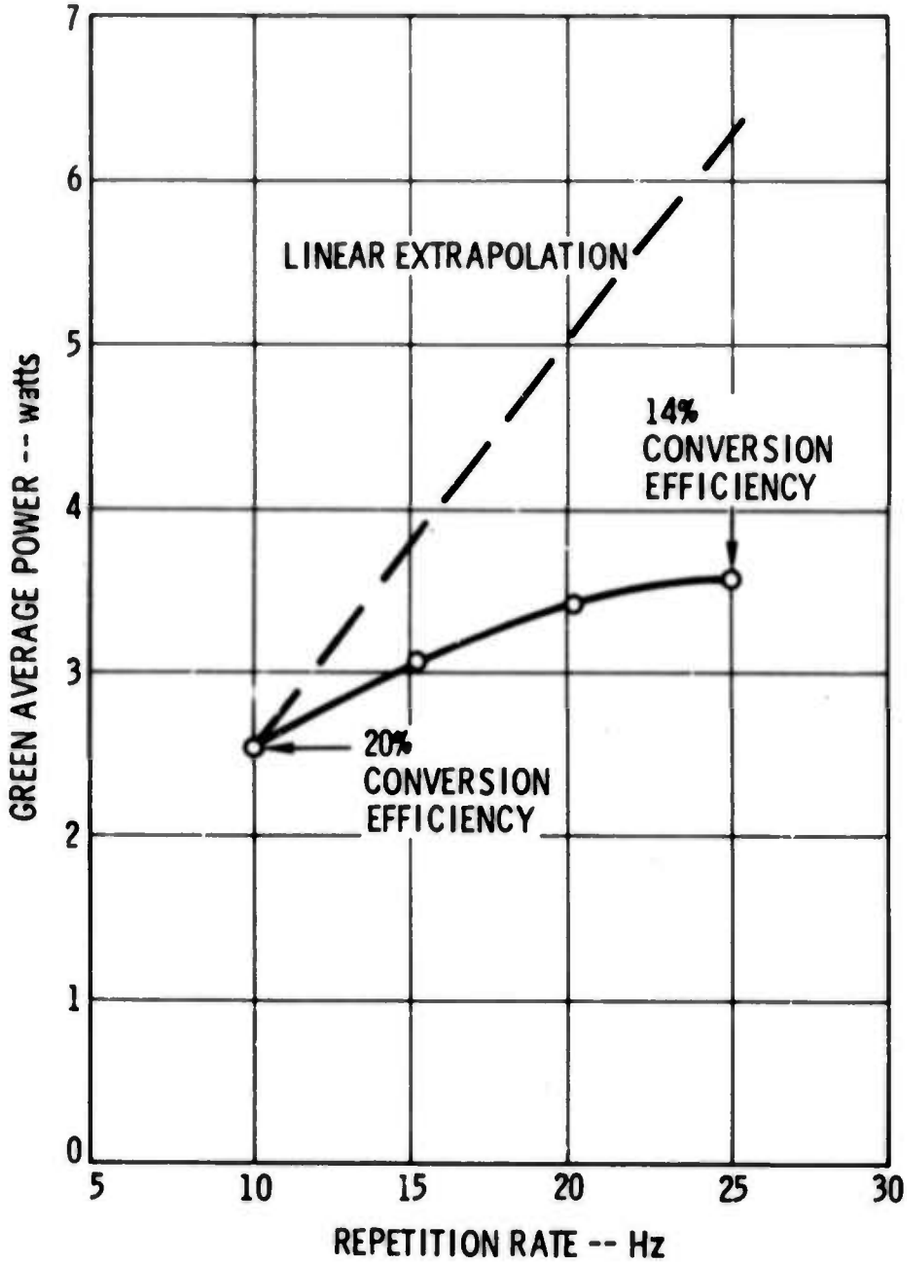

Fig. 3-3 0.53 Micron Average Output Power Versus Repetition Rate When Rotating Q-switch is Employed

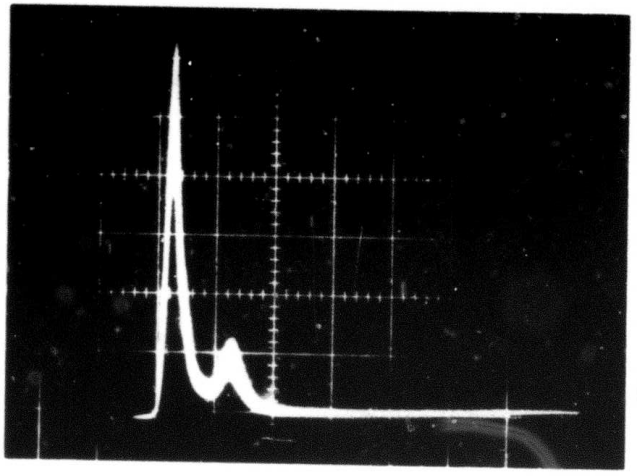

10 Hz

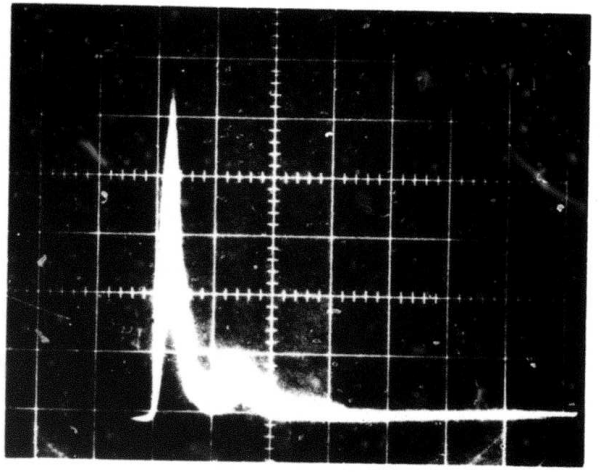

20 Hz

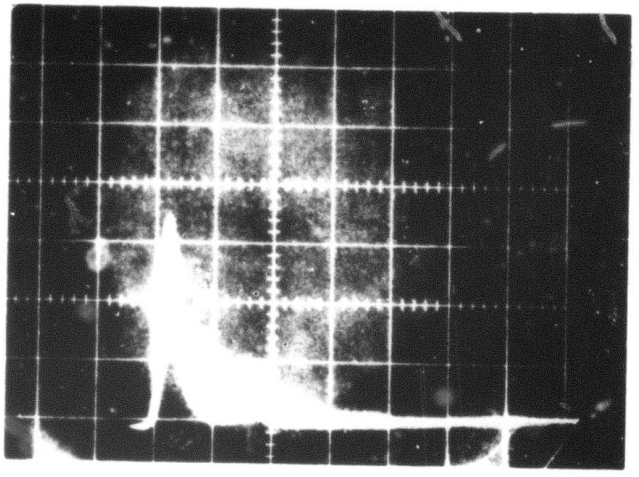

30 Hz

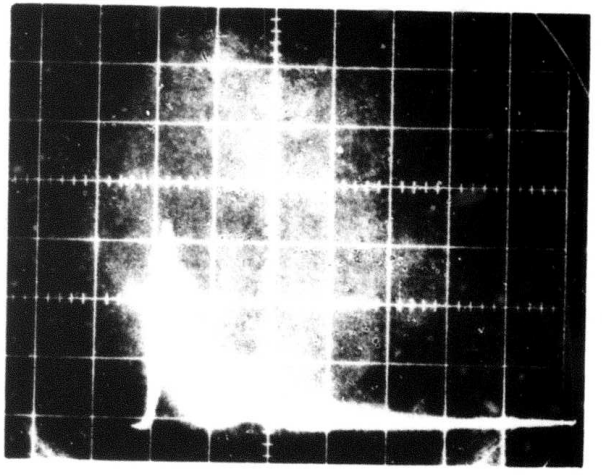

40 Hz

Fig. 3-4 Degradation of Q-switch Pulses as Repetition Rate is Increased Scale is 100 ns/division.

rotating prism Q-switch. Since the pulse length is ∿ 16 nsec for the electro-optic Q-switch as opposed to ∿ 30 nsec for the rotating prism, the power density is twice as great using the electro optic Q-switch.

The SHG results using the unfocused laser beam from the electro-optically (EO) Q-switched MOPA system are shown in Figure 3-5. At 10 Hz, the conversion efficiency is increased to ∿ 40%, about twice that with the rotating prism. In addition, no damage occurred at this conversion rate. As the repetition rate is increased to 25 Hz, some saturation is seen, but not so bad as before. Again, much of the fall off is due to depolarization in the amplifier stages. The maximum stable average power reached was 9.4 watts. For a few seconds, 10 watts could be obtained.

Unfortunately, the repetition rate could not be increased beyond 25 Hz due to power supply averate power limitations. Judging from the saturation behavior shown in Figure 3-5, it appears that green powers of 12-45 watts would be obtainable from the present system at higher repetition rates. If $Nd:YAlO_3$ were used, there would be no depolarization effects and the green would not saturate much.

After several seconds operation at 25 Hz, the CD*A crystal fractured along its length. One of these crystals is shown in Figure 3-6. The crystals when received had small cleaves along the surface, and it is believed that the large fracture occurred along one of these cleaves. We discussed this problem with Quantum Technology Ltd., and they suggested that in the future the crystals not be kept in a dry atmosphere, which accents the tendency to crack, but that the humidity be kept around 30%.

Due to saturation of the laser, we were not able to determine the maximum green average power obtainable from a single crystal. Our experiments suggest, however, that at least 15 watts could be obtained from a single crystal (assuming the 40% conversion we observed). The conversion efficiency can probably be increased further without damage, especially with the use of longer crystals and/or cleaner pump beams. An array of 4 or 5 crystals used with a fairly clean pump beam should produce in excess of 50 watts average power in the green.

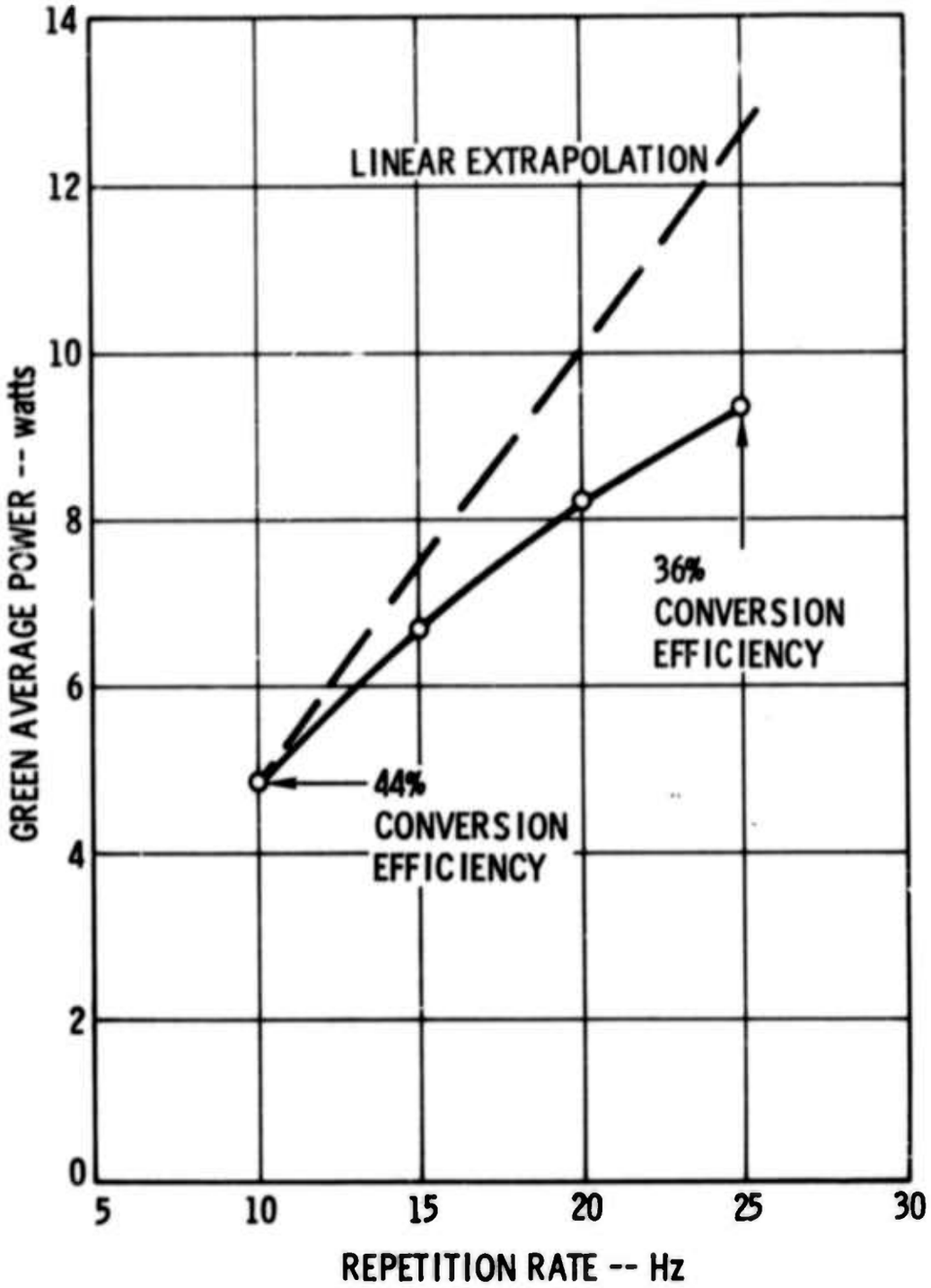

Fig. 3-5 0.53 Micron Average Output Power Versus Repetition Rate When Electro-Optic Q-Switch is Employed

Fig. 3-6 Photograph of Fractured CD*A Crystal

Section IV

SECOND HARMONIC GENERATION FROM 0.532 MICRON TO 0.266 MICRON

4.1 AMMONIUM DIHYDROGEN PHOSPHATE (ADP)

ADP is the only good candidate for frequency doubling from 0.532 micron to 0.266 micron. It is 90° phase matchable and has a high damage threshold. It is relatively transparent at both wavelengths, and is available in large size crystals of good optical quality.

Several ADP crystals were fabricated with 12 mm x 12 mm cross sections, and lengths ranging from 2 cm to 7 cm.

The biggest single problem with using ADP for a frequency doubler is its very narrow temperature half-width for phase-matching. For a 5 cm crystal, the temperature half width is 0.1°C, and to stay within 90% of the peak requires temperature control of 0.025°C. By contrast, the temperature half width of CD*A is ∿ 3° for a 2 cm crystal, more than 10 times as large as ADP.

Another problem with ADP is that it is slightly absorbing at 2662Å. This absorption causes self-heating of the crystal and considerably degrades phase-matching. In addition, as will be shown in the next section, ADP has nonlinear absorption, so that the ultraviolet absorption increases dramatically at high peak and average powers.

4.2 SHG EXPERIMENTS WITH ADP FROM 0.532 MICRON TO 0.266 MICRON

4.2.1 ADP SHG Experiments

For the first experiments, a 7 cm ADP crystal was placed in an oven and heated to just below its phase matching temperature of ∿ 52°C. The unfocused green output beam from the CD*A doubler was directed through the ADP crystal. With a green input energy of ∿ 0.5 joule/pulse at 40 Hz, the output energy was ∿ 30 mJ/pulse, giving an average power of 300 mW in the ultraviolet. When a lens was added to increase the power density, the ultraviolet output decreased, although no crystal damage occurred. This behavior is opposite to what one would theoretically expect.

Phase-matching of the ADP crystal was very sensitive. In general, phase matching was achieved by tilting the crystal very slightly off normal incidence and lowering the temperature slightly. The oven was then tilted slightly one way or the other to achieve phase matching. As phase-matching was approached, the UV power rose gradually to $\sim$ 50 mW and then suddenly jumped to 300 mW as the oven was tilted further. The power could be maintained at this level by tracking the ultraviolet power with oven tilt, until finally the UV stabilized at this level. If the pump beam was blocked momentarily and then unblocked, the UV level would return to $\sim$ 50 mW again, and the oven would again have to be tilted until the UV "latched-on".

This behavior is strongly indicative of substantial ultraviolet absorption in ADP. Since the UV output decreased with focusing of the pump, it was surmised that the smaller pump tried to generate more UV, but the UV was confined to a smaller area and somehow increased the absorption (i.e., nonlinear absorption). This in fact turned out to be the case, as will be discussed below.

Since the phase-matching half-width of the 7 cm crystal is only $\sim 0.07^{\circ}C$ and to stay within 90° of the peak requires temperature control of $\sim 0.018^{\circ}C$, it seemed very likely that UV absorption was causing local heating so that the effective crystal length was much less than 7 cm. In order to test this hypothesis, a 2 cm ADP crystal was substituted for the 7 cm crystal. The 2 cm crystal has 3.5 times the temperature half width, so that heating should not cause as much degradation as before. Since the second harmonic conversion efficiency goes as the square of the length, in the absence of absorption, one would expect far less UV from the short crystal. Instead, we obtained more UV from the short crystal. With no focusing, we obtained up to 0.1 joule pulses at 0.266 micron from 0.5 joule 0.532 micron pulses, at 10 Hz (20% conversion). Again, focusing the pump decreased the output UV power. The crystal still showed the same "latching-on" effect as phase matching was approached.

When the repetition rate of the green pump was increased beyond 10 Hz, no further increase resulted in the UV output, showing again that severe saturation was taking place, presumably due to UV absorption.

A still shorter ADP crystal, of ∿ 1.5 cm length, was tried, but produced less conversion than the 2 cm crystal. Thus it appears that ∿ 2 cm is the optimum length crystal to use for frequency doubling.

4.2.2 Nonlinear Absorption in ADP

Based on these results, we decided to measure the UV absorption of ADP. Using ∿ 300 mW in the UV from the ADP frequency doubler, we measured the UV transmission of various lengths of ADP. We were amazed to find as much as 30% absorption! When the power density was increased by focusing the UV beam, the absorption increased further. Previous transmission measurements using a Cary 14 recording spectrophotometer on crystals from the same boule had shown very little absorption in the UV. We then measured the same crystal's absorption in the UV with the 300 mW beam and with the Cary 14. The transmission for the 2 cm crystal using the Cary 14 is shown in Figure 4-1. The transmission at 0.266 micron is 86.5%. Discounting 8% loss due to Fresnel reflections, the maximum absorption is 5.5% for the 2 cm crystal. Likely the Fresnel reflection loss is slightly larger at this wavelength due to the index of refraction increasing.

Table 4-1 shows a comparison of the absorption data using the Cary 14 and the 300 mW UV beam. It is obvious from this data that ADP does indeed have nonlinear absorption. For the worst case, the absorption is 46%! These data explain the puzzling results obtained in the SHG experiments. Because of the increased absorption with focusing, no more second harmonic is generated, and, since the absorption also increases with crystal length, crystals longer than some critical length do not increase conversion efficiency. This length is determined from a tradeoff between increasing conversion efficiency with increasing length and increasing absorption with icnreasing length. As mentioned above, at the power levels used in these experiments, a crystal length of ∿ 2 cm proved to be optimum.

Similar absorption effects to these were reported by Dowley[4] who used ADP to generate 2573Å from an argon laser. He measured increased losses of ∿ 4% in 5 cm crystals at UV power levels of ∿ 400 mW from a cw beam. We have measured much greater absorptions than this using high peak power pulses, rather than cw pumping. However, Yarborough and Massey[5] noticed no such

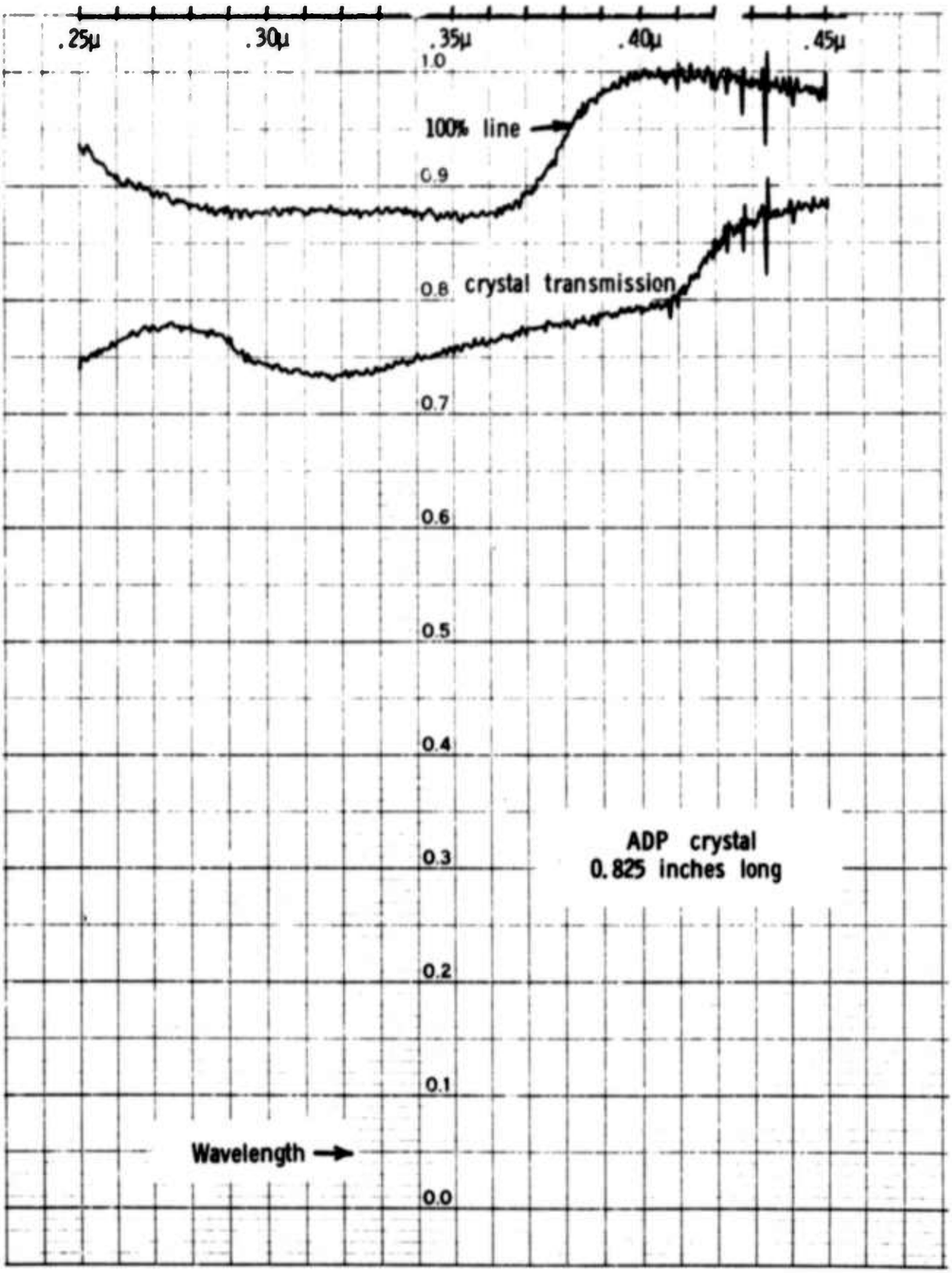

Fig. 4-1 Spectral Transmission of 2 cm Long ADP Crystal

Crystal Length	Cary 14 Transmission(%)	Transmission of 300 mw UV beam unfocused		Transmission of 300 mw UV beam focused	
		∥ c axis	⊥ c axis	∥ c axis	⊥ c axis
2.1 cm	86.5	78	73	66	60
2.8 cm	not measured	64	62	53	49
5 cm (different boule)	not measured	70	66	53	46

Note: All transmission data are uncorrected for Fresnel reflection losses of ∿ 8%.

Table 4-1 Transmission of various ADP crystals under various conditions

severe problems using roughly the same power densities as here, but with only 30 mW average power in the UV. They did, however, see only 20% conversion using a 5 cm crystal. The data presented in Table 4-1 on the 5 cm crystal was in fact taken with this same crystal, which can be seen to have less absorption than the present crystal, but the absorption still reaches almost 50% in some cases. Dowley[4] suggests that this absorption is due to impurities in ADP. This may be true, since in general impurities are purposely added to ADP in order to grow large crystals. He also measured increased pump absorption in the presence of high UV conversion. We made no measurements of the green absorption in the presence of UV, but it is likely that this was also occurring in our experiments.

Section V

0.266 MICRON PUMPED VISIBLE PARAMETRIC GENERATOR

5.1 DESIGN CONSIDERATIONS

Based on earlier work of Yarborough and Massey[5], it was anticipated that a second ADP crystal could be pumped by the 0.266 micron output to give a parametric generator tunable over the visible. In their earlier experiments, the 30 mW (30 Hz) UV beam was focused into an uncoated 5 cm long ADP crystal. The end faces were fabricated parallel, and formed a low Q resonator for the parametrically generated signals. The oscillator was tuned over the visible spectrum, as shown in Figure 5-1, and conversion efficiencies of ∿ 30% were obtained. It was thus thought possible to use the 4 watt UV beam which was to be produced on this program as a pump to produce visible outputs in excess of 1 watt. Due to the problems with ADP discussed in Section 4, only 1 watt of UV was available. Using this one watt pump beam, it still seemed feasible to produce outputs of ∿ 300-400 mW from the parametric generator. This did not turn out to be the case, as explained in the next section.

5.2 ADP PARAMETRIC GENERATOR EXPERIMENTS

The UV beam from the ADP frequency doubler was used to pump a second 5 cm ADP crystal oriented for parametric generation. The end faces of the crystal were polished parallel to form a resonator, and the crystal was mounted in an oven for temperature tuning the output wavelength. With a pump average power of 600 mW at 10 Hz, visible parametric generation was observed. It was tuned over the same range shown in Figure 5-1. Figure 5-2 shows a schematic diagram of the entire experiment.

The conversion efficiency from UV to visible was very poor. At most, 20 or 30 mW was obtained in the visible, and the generator ran within a ring, with no visible output in the center of the beam. When the pump beam was blocked for a few seconds and then unblocked, the generator emitted a round beam, but the middle again went out in a few seconds. Focusing the UV beam and using longer or shorter crystals did not substantially change the operation of the parametric generator. We believe that the nonlinear ADP absorption described in Section 4.2.2 is responsible for the poor parametric

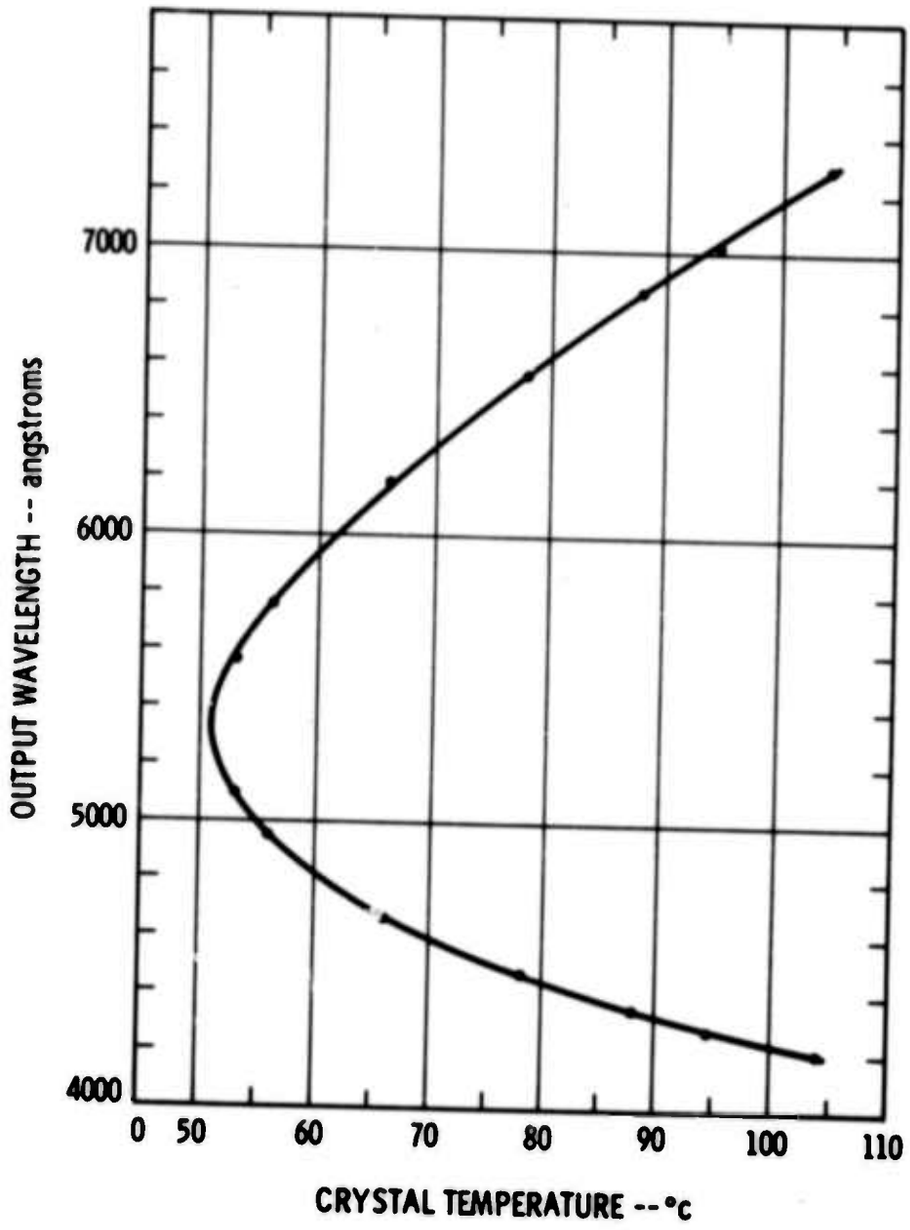

Fig. 5-1 Tuning Curve Obtained in ADP Parametric Generator Experiment

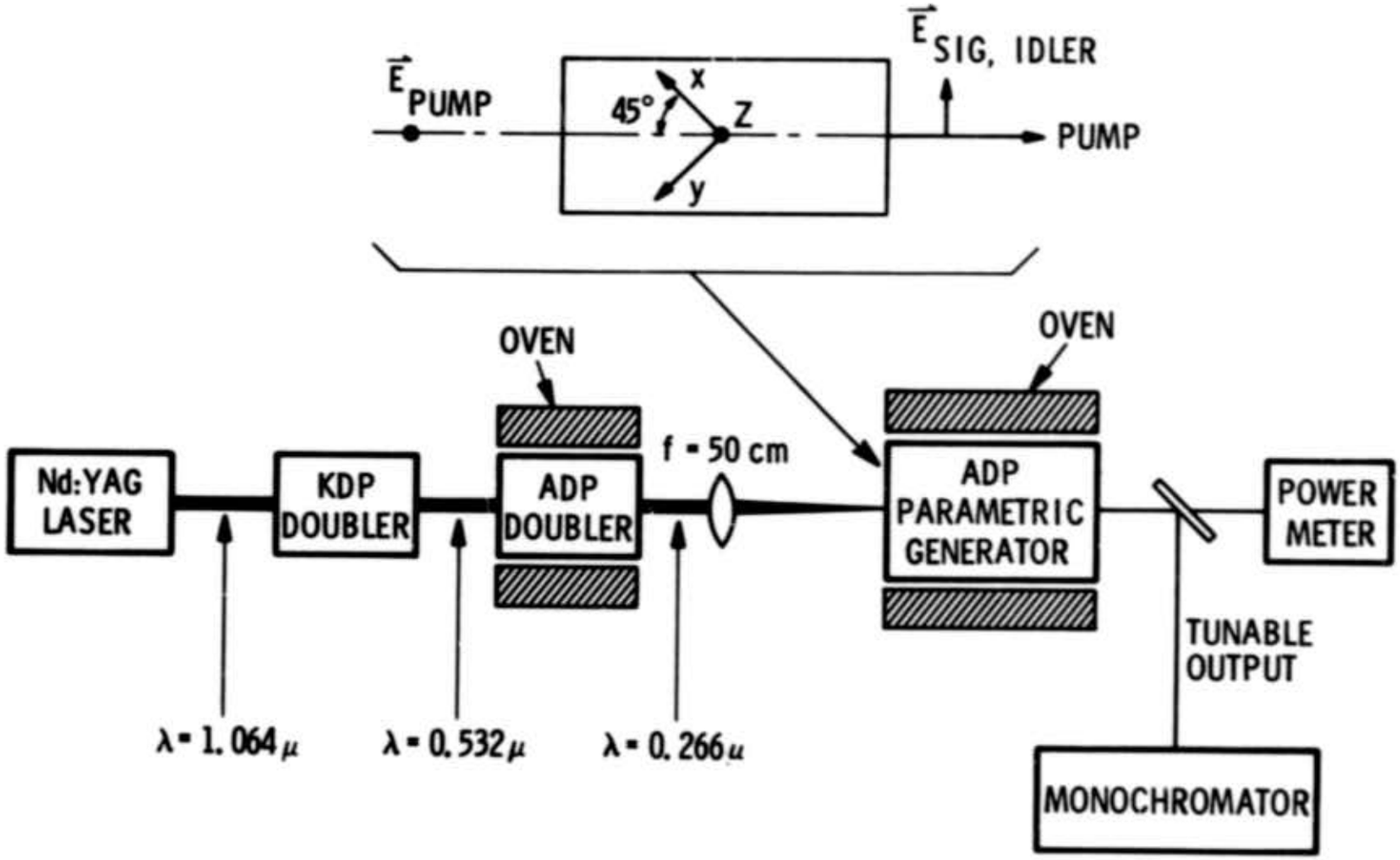

Fig. 5-2 Schematic Diagram of ADP Parametric Generator Experiment

generation efficiency which we observe. The 0.266 micron pump is absorbed in the ADP by this nonlinear absorption rather than being available to produce a signal and idler.

Section VI

SUMMARY AND CONCLUSIONS

Substantial progress toward efficient, high average power (> 10 watts) second harmonic generation of Nd:YAG lasers has been made on this program. It has been demonstrated that prolonged operation without damage at > 40% conversion efficiency and average powers in the 10 watt area are possible. Use of longer crystals or a cleaner pump beam would enable conversion efficiencies in the 60% - 70% range with no damage. Small residual absorption in CD*A at 1.06 micron causes degradation of phase matching as the pump average power is increased, and the reduction of this absorption (if possible) would increase the maximum average power obtainable in the green. From the experiments performed here, it appears that average green powers of 15 watts should be obtainable from 2 cm long presently available CD*A crystals. Due to thermal depolarizing of the YAG pump beam at high average powers, we were not able to completely saturate the green output of the CD*A crystals. If $YAlO_3$ or some other similar birefringent host becomes available so that depolarization does not occur, the actual limit of the crystals can be found. Another alternative would be to use one more YAG amplifier with the present system, thus increasing the energy/pulse.

Average power-conversion efficiencies of 20% with ultraviolet (2662Å) average powers of one watt have been achieved in ADP with no damage. Large nonlinear absorption in ADP at 2662Å were observed, and this absorption prevented the generation of higher average powers in the ultraviolet. It has been suggested that this absorption is due to impurities in ADP.

High average power operation of an ADP parametric oscillator does not appear feasible at this time due to the UV nonlinear absorption in ADP. The use of mirrors around the parametric generator would increase the efficiency of the device considerably, but at this time there are no mirrors which will withstand the high power UV beams used in these experiments.

Section VII

REFERENCES

1. M. Bass and M. S. Weber, Appl. Phys. Lett. 17, 395 (1 Nov. 1970).

2. G. A. Massey and J. M. Yarborough, Appl. Phys. Lett., 18, 576 (15 June 1971).

3. J. D. Foster and L. M. Osterink, J. Appl. Phys., 41, 3656 (August 1970).

4. M. W. Dowley, Appl. Phys. Lett., 13, 395 (1 Dec. 1968).

5. J. M. Yarborough and G. A. Massey, Appl. Phys. Lett. 18, 438 (15 May 1971).